Research Square

Preprints are preliminary reports that have not undergone peer review.
They should not be considered conclusive, used to inform clinical practice,
or referenced by the media as validated information.

The seasonal variation of rainfall in East Africa: How well is it represented in the CORDEX-CORE simulations?

Wilhelm May

wilhelm.may@mgeo.lu.se

Clough Yann

Research Article

Keywords: Rainfall, Seasonal variation, Rainy seasons, East Africa, Regional climate models

Posted Date: November 23rd, 2026

DOI: https://doi.org/10.21203/rs.3.rs-11549288/v1

License: This work is licensed under a Creative Commons Attribution 4.0 International License.
Read Full License

Additional Declarations: No competing interests reported.

The seasonal variation of rainfall in East Africa: How well is it represented in the CORDEX-CORE simulations?

by

Wilhelm May and Yann Clough

Department of Earth and Environmental Sciences, Lund University, Lund, Sweden

Submitted to *Theoretical and Applied Climatology*: October 29, 2026

Corresponding author:

Dr. Wilhelm May, Sölvegatan 12, 223 62 Lund, Sweden,

e-mail: wilhelm.may@mgeo.lu.se, orcid: 0000-0002-4933-3565

Co-author:

Prof. Yann Clough, e-mail: yann.clough@mgeo.lu.se, orcid: 0000-0002-2901-7602

Abstract

Realistic representations of the seasonal variation of rainfall in regional climate simulations are crucial for assessing the potential socio-economic impacts of future climate changes in areas that strongly rely on seasonally reccurring rainfall. Yet assessments of how well this is simulated by regional climate models (RCMs) is often lacking. Here, we investigated the extent to which regional climate simulations within the CORDEX-CORE experiment for Africa realistically represent the seasonal variation of rainfall in East Africa. Specifically, we compare the performance among three different RCMs, either forced with observed lateral meteorological boundary conditions or with data from global climate simulations with three different models. The simulations forced with ERA-Interim reanalyses indicated that the RegCM RCM best simulates the phase, shape and magnitude of the climatological annual cycle of daily rainfall in East Africa. The simulations driven by the global climate models (GCMs) showed that only the boundary conditions from the MPI-ESM GCM enable realistic simulations of the seasonal variation of rainfall in East Africa by the RCMs. For the boundary conditions from the two other GCMs, the regional climate simulations failed to capture the observed dominance of two rainy seasons over parts of the Horn of Africa and in the central tropics. Each of the RCMs is characterized by model- and location-specific deviations from observations for the onset, cessation and length of the rainy seasons. These results provide guidance in choosing viable regional climate simulations for use in climate impact and adaptation research in East Africa.

Keywords: Rainfall, Seasonal variation, Rainy seasons, East Africa, Regional climate models

1. Introduction

With its location around the equator, the occurrence of rainfall in East Africa is characterized by marked seasonality. Regions near the equator and the Horn of Africa have two rainy seasons in autumn and spring, while regions further away from the equator have one rainy season centred around local summer (Dunning et al. 2016). The dependence of agricultural activities on the occurrence of rainfall (Nakawuka et al. 2018) makes agriculture in the region extremely vulnerable to variations in rainfall, such as the timing (onset and cessation), the length and the amount of rainfall accumulated during the wet seasons as well as prolonged dry spells during vulnerable crop growth stages (Porkka et al. 2021). With the ongoing and expected future climate change the total amount of precipitation increases in some parts of the globe and decreases in others (IPCC 2021), and the intensity and frequency of various types of weather and climate extremes have increased and will continue to do

so, accompanied by an overall strengthening of climate variability (Seneviratne et al. 2021). These changes in climate are already having and will have even stronger adverse effects on agriculture by decreasing yields, particularly in the tropics, unless efforts to adapt the agricultural practices to the changing climate are undertaken (Challinor et al. 2014). Hence, investigating the potential effects of future changes in climate on agricultural production in East Africa is essential for assessing the possible threats to food security in the region (e.g., Ericksen et al. 2009).

Given the dependence on the occurrence of rainfall, it is imperative that the climate models providing these scenarios represent the seasonal variation of rainfall in East Africa realistically, and evaluations are needed to allow informed choices of suitable model simulations. The global climate models (GCMs) contributing to the Coupled Model Intercomparison Project Phase 5 (CMIP5), for instance, often have problems with simulating the progression and timing of the wet seasons in various parts of Africa (Dunning et al. 2017). This includes East Africa, where the GCMs show a timing bias with, for instance, the simulated onset of the rainy season in boreal spring over the Horn of Africa being 20 days late on average.

Simulations with regional climate models (RCMs) not only provide climate information at much finer spatial scales than GCMs but also give significant added value in regions with variable orography, land-sea and other contrasts, as well as in capturing sharp, short-duration and extreme events (e.g., Rummukainen 2016; Giorgi 2019). Dynamical downscaling also gives significant added value in the provision of regional-scale information, including climate change projections, that is essential for assessing the potential impacts of future climate change and the adaptation to these impacts. The characteristics of a climate simulation with an RCM in a domain are affected by how well the GCMs that provide the atmospheric boundary forcing for the RCM represent the large-scale atmospheric circulation or the states of the ocean basins in the regions surrounding the domain (e.g., Karypidou et al. 2023; Palmer et al. 2023b). This might call for considering only those regional climate simulations, where the driving GCMs simulate the governing aspects of the large-scale circulation for the domain with a certain degree of realism. Palmer et al. (2023b), for example, undertook a selection of the GCMs from the Coupled Model Intercomparison Project Phase 6 (CMIP6) based on their realism for simulating various aspects of the large-scale atmospheric circulation and of the state of the North Atlantic Ocean known to have strong effects on the climate in Europe.

The international COordinated Regional Downscaling EXperiment (CORDEX) program aims

at generating large ensembles of continental-scale climate projections covering most land areas (e.g., Giorgi et al. 2009; Jones et al. 2011; Giorgi and Gutowski 2015). Weaknesses of this approach have been the heterogeneity of the ensemble size for the different domains, differences in the simulation protocol (e.g., the choice of the driving GCMs) and the relatively low resolution. This has hampered a consistent assessment of these downscaled projections across the different regions and inhibited the coordinated use of the projections for impact studies in most regions (Giorgi et al. 2022). To provide a homogenous set of climate projections for all domains, Gutowski et al. (2016) proposed the CORDEX-CORE (Coordinated Output for Regional Evaluations) initiative, using a core set of RCMs driven by a common set of GCMs, following the same simulation protocol for each domain and with a resolution of 10-20 km. Based on the simulations of the CORDEX-CORE experiment, a range of scientific questions have been addressed (e.g., Ashfaq et al., 2021; Coppola et al. 2021, Giorgi et al. 2021, Teichmann et al. 2021). To our knowledge, these simulations have not been studied to determine the suitability of the climate simulations with specific combinations of RCMs and the driving GCMs for assessing the potential impacts of future climate change in East Africa.

In this study we assess the extent to which the three RCMs contributing to the CORDEX-CORE experiment covering Africa represent the seasonal variation of rainfall in East Africa in accordance with observations of daily rainfall. This was done for the stream of RCM simulations driven by lateral boundary conditions from the ERA-Interim reanalyses and for the stream of RCM simulations driven by lateral boundary conditions from the three different GCMs considered in CORDEX-CORE. In the first case, deviations from the observations are only due to the characteristics of the specific RCM, while in the second case, we hypothesized that the representation of the large-scale atmospheric flow around Africa and remote forcings such as the Indian Ocean Dipole (IOD) and the El Niño/Southern Oscillation phenomenon (ENSO; e.g., Nicholson 2017; Palmer et al. 2023a), in the selected GCMs have a strong influence on the simulation of the seasonal variation of rainfall in East Africa by the RCMs.

2. Data and methods

2.1 Observational data

As main observational data of daily precipitation, we used version 2.0 of the Climate Hazards group InfraRed Precipitation with Stations (CHIRPS) dataset for Africa (Funk et al. 2015). The dataset is based on previous approaches of advanced interpolation techniques and high-resolution precipitation

estimates based on infrared Cold Cloud Duration observations covering long records. As an alternative daily precipitation dataset, version 3.1 of the Tropical Applications of Meteorology based on SATellite data and ground-based observations (TAMSAT) dataset for Africa was considered (Maidment et al. 2014; Tarnavsky et al. 2014; Maidment et al. 2017). The long periods, the high spatial and temporal resolution and short latency make these two datasets particularly suitable for climate monitoring. Evaluations for East Africa (Dinku et al. 2018; Gebrechorkos et al. 2018) and Africa (Dosio et al. 2021) have demonstrated the high quality of these two datasets regarding the statistics of daily precipitation.

The CHIRPS data are available at a high resolution of 0.05° and a low resolution of 0.25°, starting in 1981 and extending to the present day. The TAMSAT data are available at a high resolution of 0.0375° and several lower resolutions, including 0.25°, starting in 1983 and extending to the present day. In this study, we used both observational datasets at the lower resolution of 0.25° to match the resolution of the climate simulations.

2.2 CORDEX-CORE climate simulations

The CORDEX-CORE initiative was proposed by Gutwowski et al. (2016) to provide a homogenous set of climate projections for various domains using a core set of RCMs driven by a common set of GCMs, following the same simulation protocol for each domain. CORDEX-CORE consists of three RCMs (one of them joining later) downscaling three GCMs from CMIP5 for two greenhouse gas (GHG) concentration pathways for nine domains at a resolution of about 25 km (Giorgi et al. 2022). The CORDEX-CORE protocol consists of two simulation streams. In the first, the model evaluation stream, the RCMs were forced with a reanalysis of observations for the historical period. In the second, the RCMs were driven by three selected GCMs for simulations covering the historical period and the 21st century under two different GHG emission scenarios.

The three RCMs providing simulations for the CORDEX-CORE experiment are RegCM (Giorgi et al. 2012), REMO (Jacob et al. 2012) and COSMO-CLM (Sørland et al. 2021). The fourth-generation version of the RegCM regional climate modelling system (Giorgi et al. 2012) developed at the Abdus Salam International Centre for Theoretical Physics is used. The model includes multiple options for the physical parameterizations, and for each domain a specific physics scheme was selected, optimizing the model performance for the main climate variables (Coppola et al. 2021). The REMO version from 2015, which is developed at the Climate Service Center Germany, is based on

the dynamics of the German Weather Service weather prediction model ('Europamodell') and the physics of the ECHAM 4.5 GCM (Jacob et al. 2012). For all domains the same physics scheme was used, and only the values of some parameters were adjusted to account for the specific climate conditions for a domain (Remedio et al. 2021). COSMO-CLM is developed by the Climate Limited-area Modelling (CLM) community (Sørland et al. 2021). It is the climate version of the COSMO model, which itself is developed based on the 'Lokal Modell' of the German Weather Service. Version 5 of the regional climate modelling system is used in CORDEX-CORE for Africa (Sørland et al. 2021). The three RCMs are referred to as RegCM, REMO and CCLM in the following.

Three GCMs from CMIP5 were chosen to force the RCMs in CORDEX-CORE, i.e., HadGEM2-ES (Jones et al. 2013), MPI-ESM (Giorgetta et al. 2013) and NorESM1-M (Bentsen et al. 2013). These GCMs were selected because they were among the models performing best over the CORDEX-domains and because they roughly span the range of climate sensitivity of the CMIP5 ensemble (Giorgi et al. 2021). The restriction to three GCMs accounted for the available computational and human resources needed to perform the set of simulations. The GCM simulations (as well as the atmospheric reanalysis) provided time-dependent horizontal boundary conditions for the horizontal wind components, temperature and water vapour across the atmosphere and surface pressure (or related variables for some models) at 6-hourly intervals. Sea surface temperature (SST) was interpolated from the GCMs (or prescribed from observations), while each RCM had its own constant land-surface conditions. The GHG concentrations in the RCMs were prescribed according to observations for the historical period. The three driving GCMs are referred to as HadGEM, MPI-ESM and NorESM in the following.

Table 1 gives an overview of the RCM simulations for Africa in CORDEX-CORE considered in this study. On one hand, there is the stream of RCM simulations forced with the ERA-Interim reanalyses (Dee et al. 2011) for the historical period, the evaluation simulation (EVAL). Considering complete years only, the three RCMs have the common period 1980-2009. On the other hand, there is the stream of RCM simulations driven by the three GCMs for the historical period (HIST). Note that in the case of the MPI-ESM, RegCM is driven by a simulation with another version of the GCM, i.e., the MR version, which differs from the LR version by the number of vertical levels in the atmosphere (95 vs. 47) and the structure of the horizontal grid of the ocean model (Giorgetta et al. 2013). In this case, the three RCMs have the common period 1970-2014 with complete years. To match the grid of the two observational datasets, the data of daily precipitation for the RCM

153 simulations with a resolution of 0.225° were interpolated to a 0.25° regular grid prior to the analysis.

154 2.3 Seasonal variation of rainfall

155 For each dataset and each grid point, the climatological annual cycle of daily precipitation was
156 computed as the long-term means of the daily precipitation for each calendar date, including February
157 29. The local seasonal variation of the climatological annual cycle was then derived by estimating the
158 smoothed annual cycle by means of a harmonic analysis as described in May et al. (1992). Where the
159 RCM simulations did not follow the full calendar year by either not considering the leap day or having
160 months with a fixed length of 30 days, the climatological annual cycles were extended to 366 days
161 before the harmonic analysis by filling the gaps using the data from the adjacent dates.

162 The seasonal variation of rainfall was determined by the phase as well as by the shape and
163 magnitude of the climatological annual cycle of daily rainfall. We constructed Taylor diagrams to
164 evaluate the quality of the simulation of these aspects of the annual cycle (Taylor 2001). The
165 correlation presented in such a diagram indicates the phase error between simulation and observation,
166 while the centred root-mean-square (RMS) deviation summarizes the differences between the
167 climatological values of daily rainfall between simulation and observation after the respective annual
168 mean values have been subtracted.

169 2.4 Rainy seasons

170 The climatological rainy seasons were identified following the method outlined in Dunning et al.
171 (2016). For each dataset and grid point, the dominant harmonic representing either the annual or the
172 semi-annual variation of the climatological annual cycle of precipitation, was determined. In cases,
173 where either the first or the second harmonic was the dominant one, the onset and cessation dates for
174 the annual and the biannual regimes were derived using the method described in Dunning et al.
175 (2016). Different from Dunning et al. (2016), the onset and cessation dates were not computed for
176 individual years (and then averaged) but from the climatological annual cycle to account for the strong
177 interannual variability of the onset and cessation dates. In addition to the onset and cessation dates,
178 we present estimates of the length to characterize the dominant rainy seasons. The first of two rainy
179 seasons in East Africa in boreal spring is sometimes referred to as the “long rains” and the second
180 one in boreal autumn as the “short rains” (e.g., Nicholson 2017).

181 2.5 Study region

The study region comprises 9 countries in East Africa, reaching from Eritrea in the north to Tanzania in the south and from Somalia in the east to Rwanda and Burundi in the west (Fig. 1; note that the border between Eritrea and Ethiopia is missing on the maps). The region is dominated by the Ethiopian and the East African plateau, with large areas exceeding elevations of 2000 m in the Ethiopian and the Kenyan highlands and including the highest peaks in Africa, which exceed 4000 m in various places and reach almost 6000 m for Mount Kilimanjaro. The coastal regions are covered mainly by lowland plains. Two parallel rift valleys run through the region, the Eastern Rift Valley extends from the Red Sea southwards across the Ethiopian and Kenyan highlands and continues into Tanzania, while the Western Rift Valley curves along the western borders of Uganda, Rwanda, Burundi and Tanzania. Between the two rift valleys lies Lake Victoria, reaching into Uganda, Tanzania and Kenya.

3. Results

3.1 Observations

The CHIRPS observational data reveal that East Africa is characterized by one dominant rainy season in the regions off the equator except for the Horn of Africa (Figs. 2a-c). These regions include Eritrea and the northern part of Ethiopia, the northern part of Uganda and the northeastern part of Kenya, Burundi, Tanzania extending across the border into southern Kenya and a narrow strip along the coast of southern Somalia. Two rainy seasons dominate over the Horn of Africa, extending into the eastern part of Kenya, over the Kenyan highlands as well as along the equator over southern Uganda, northern Rwanda, Lake Victoria and the very western part of Kenya (Figs. 2d-i).

For one rainy season, the onset falls into boreal spring (Fig. 2a) and the cessation into boreal autumn in the regions in the Northen Hemisphere and over the coastal strip in southern Somalia (Fig. 2b). In the Southern Hemisphere the onset of the annual rainy season falls into boreal autumn and the cessation into boreal spring. In the regions near the equator the onset of the annual rainy season is earlier and the cessation later than in the regions further away, leading to an annual rainy season of about six months near the equator compared to four to five months in southern Tanzania and the northwestern part of Ethiopia (Fig. 2c).

For the first of two rainy seasons, the onset varies between February in the regions near the equator and April over the northern part of Somalia (Fig. 2d). The cessation, on the other hand, shows

only little regional variation, with this rainy season typically ending in June (Fig. 2e). Only over a narrow coastal strip in southern Somalia, the first rainy season lasts until August. This strip and northern Rwanda are the areas, where this rainy season lasts for about 100 days compared to 50 to 80 days in the other regions (Fig. 1f). The second rainy season is generally slightly shorter than the first one except for southern Uganda with a length of about 120 days (Fig. 2i). The latter is due to an early onset of this rainy season in August compared to October in the other regions centred around the equator (Fig. 2g). Over the Horn of Africa, the onset of the second rainy season varies between August in the northern part of the region and October in the southern part and the cessation varies between November and December, respectively (Fig. 2h).

The local or regional characteristics of the rainy seasons can depend on the choice of the observational dataset used as reference, possibly introducing some uncertainty to the quality assessment of model simulations (e.g., Salami 2025). Compared to CHIRPS, the TAMSAT dataset is characterized by a very similar geographical distribution of the areas with one and two dominant rainy seasons but some local and regional differences in the characteristics of the rainy seasons (Fig. S1). For the first of two rainy seasons, however, TAMSAT shows an earlier onset of up to several weeks over most of the area (Fig. S1d) and a later cessation (Fig. S1e), resulting in a longer rainy season of up to several weeks over most of the area (Fig. S1f).

3.2 RCM simulations forced with ERA-Interim

3.2.1 Seasonal variation of rainfall

The Taylor diagrams with CHIRPS as reference data indicate that all three RCMs are better at capturing the climatological annual cycle of daily rainfall in the areas with one dominant rainy season than in the areas with two rainy seasons (Figs. 3a-c). This is particularly the case for the phase of the annual cycle (measured by the correlations; Figs. 3d-f) and to a lesser extent for the magnitude (measured by the centred RMS deviations; Figs. 3g-i). For the areas with one rainy season the correlations are typically in the range between 0.4 and 0.9 but in the range between 0.2 and 0.7 for the areas with two rainy seasons (Figs. 3d-f), with medians between 0.67 and 0.80 for one rainy season and between 0.46 and 0.68 for two rainy seasons, respectively (Table 2). The RMS deviations are typically in the range between 0.5 and 1.2 for the areas with one rainy season and between 0.7 and 1.4 for the areas with two rainy seasons (Figs. 3g-i). In this case the medians are between 0.73 and 0.84 for one rainy season and between 0.82 and 0.96 for two rainy seasons, respectively (Table

241 2).

242 The diagrams reveal that RegCM is best among the three RCMs at representing the
243 climatological annual cycle of daily rainfall in East Africa (Figs. 3a-c). This is particularly the case
244 for the phase of the annual cycle, especially for the areas with two rainy seasons but also for the areas
245 with one rainy season (Figs. 3d-f). For RegCM the correlations are mostly in the range between 0.5
246 and 0.8 for two rainy seasons and between 0.7 and 0.9 for one rainy season, which is markedly higher
247 than for the two other RCMs. Consistent with this, the medians are highest for RegCM, with 0.68
248 compared to 0.46 for REMO and 0.53 for CCLM for two rainy seasons and 0.80 compared to 0.67
249 for CCLM and 0.67 for REMO for one rainy season (Table 2). For the areas with two rainy seasons
250 CCLM is somewhat better than REMO, which shows a relatively large fraction of correlations below
251 0.4 (Fig. S2f). Also for the RMS deviations RegCM is better than the two other RCMs, again,
252 especially for the areas with two rainy seasons (Figs. 3g-i), with a median of 0.82 compared to 0.93
253 for CCLM and 0.98 for REMO (Table 2). The values of the medians for the two rainy seasons indicate
254 that CCLM is somewhat better than REMO at simulating the seasonal variation of daily rainfall in
255 East Africa.

256 These finding are confirmed when TAMSAT is used as reference data. The Taylor diagrams
257 (Figs. S2a-c) reveal many of the same characteristics as for the CHIRPS dataset (see Figs. 3a-c). A
258 notable difference, however, can be seen for RegCM, where the highest correlations are somewhat
259 lower in the areas with two rainy seasons with values of up to 0.78 (Fig. S2b) compared to values of
260 up to 0.85 for CHIRPS (see Fig. 3b). This is also revealed in the corresponding histogram with a
261 narrower distribution with the highest values cut off in the area with two rainy seasons for TAMSAT
262 (Fig. S2e) compared to CHIRPS (see Fig. 3e) and by the corresponding medians of 0.62 (Table S1)
263 and 0.68 (Table 2), respectively. As for the CHIRPS data, the values of the medians also confirm the
264 tendency that RegCM is best at simulating the seasonal variation of rainfall in East Africa, especially
265 in the areas with two rainy seasons, while CCLM is somewhat better than REMO (Table S1). An
266 exception, however, is found for the centred RMS deviation for one rainy season with a rather low
267 median of 0.77 for REMO, compared to 0.78 for RegCM and 0.86 for CCLM.

268 Because RegCM clearly simulates the seasonal variation of daily rainfall in East Africa most
269 realistically when the boundary conditions originate from observational data, we chose to focus on
270 the simulations with RegCM in the following and present corresponding results for CCLM and
271 REMO in the supplementary material.

3.2.2 Characteristics of rainy seasons

Compared to the CHIRPS dataset, the simulation with RegCM driven by ERA-Interim represents the overall structure of the seasonal variation of rainfall in East Africa very well, with a good correspondence of the areas with one and two dominant rainy seasons with the observations (e.g., Fig. 4a). The simulation, though, tends to extend the area with two dominant rainy seasons into the areas with one rainy season in the observations (see Fig. 2a).

For one rainy season, RegCM is characterized by an earlier onset over the Ethiopian highlands and northeastern Tanzania and a later onset over the Western lowlands west of the Ethiopian highlands and in the region east of the Ethiopian Rift Valley as well as in northern Uganda and southern Tanzania (Fig 4a). The RCM shows a general tendency of a later cessation in regions with an earlier onset and an earlier cessation in regions with a later onset (Fig. 4b). As a consequence, the length of the rainy season is extended by about three to five weeks over the Ethiopian highlands and by about two to three weeks over northeastern Tanzania but reduced by three to five weeks over the Western lowlands and in the region east of the Ethiopian Rift Valley and by about two to three weeks in Rwanda and Burundi as well as over northwestern and southern Tanzania (Fig. 4c).

For the first of two rainy seasons, RegCM is characterized by a later onset of the rainy season by about one to three weeks in all areas except for southern Uganda (Fig. 4d). The cessation is earlier over southern Uganda and the northern part of Lake Victoria, in the coastal region of southern Somalia and over the northeastern part of the Horn of Africa and later over southern Ethiopia, eastern Kenya and the southern part of Somalia away from the coast (Fig. 4e). These are the only regions with a longer rainy season in the simulation, and the length of the rainy season is reduced over most of East Africa, especially over southern Uganda and the northern part of Lake Victoria, in the coastal region of southern Somalia and over the northeastern part of the Horn of Africa by about three to five weeks (Fig. 4f). In contrast, the length of the second rainy season is increased over most of East Africa, e.g., over the Horn of Africa, the northern part of Lake Victoria and western Kenya, and only reduced in southern Uganda and several small regions in southern Ethiopia and Kenya (Fig. 4i), mainly due to a later and earlier cessation, respectively, in the corresponding regions (Fig. 4h).

Comparing the simulation with RegCM forced with ERA-Interim to the TAMSAT dataset shows very similar deviations from the observations, regarding both the geographical distributions and the magnitudes (Fig. S3). For the first of two rainy seasons, however, using TAMSAT as

reference data enhances the delay in the onset of the rainy season by up to several weeks (Fig. S3d) and, thus, the shortening of the rainy season by up to several weeks over most of the area (Fig. S3f).

Also for the simulations with CCLM and REMO, the characteristics of the rainy seasons show some distinctive deviations from the observations (Figs. S4, S5). Overall, the magnitudes of the local and regional differences from the observations are comparable for the different RCMs but the varying geographical distributions indicate some specific signatures for each of the RCMs. REMO sticks out as the simulation does not show two dominant rainy seasons in the southern part of Somalia (e.g., Fig. S5a).

3.3 RCM simulations forced with GCM simulations

3.3.1 Seasonal variation of rainfall

The Taylor diagrams clearly reveal that RegCM best represents the climatological annual cycle of daily rainfall in East Africa in the case that the boundary forcing originated from MPI-ESM (Figs. 5a-c). This is particularly the case for the phase of the annual cycle in the areas with two dominant rainy seasons (Figs. 5d-f). When driven by MPI-ESM, the correlations are mainly in the range between 0.4 and 0.7 (Fig. 5e) but between 0.0 and 0.4 for HadGEM (Fig. 5d) and between 0.1 and 0.5 for NorESM (Fig. 5f) for the case of two rainy seasons. In accordance with this, the corresponding median is much higher (0.56) for MPI-ESM than for HadGEM with 0.20 and NorESM with 0.28 (Table 2). Also for the centred RMS deviations, the simulation forced with MPI-ESM is clearly better than the two other simulations (Figs. 5g-i). For two rainy seasons, the RMS deviations mainly cover the range between 0.7 and 1.1 (Fig. 5h) with a marked maximum at about 0.8 for MPI-ESM but higher and much broader ranges between 0.8 and 1.6 for HadGEM (Fig. 5g) and NorESM (Fig. 5i), again underlined by the values of the medians with 0.92 for MPI-ESM and about 1.40 for the two other GCMs (Table 2). The quality of the simulation forced with MPI-ESM is close to the simulation with RegCM driven by ERA-Interim (see Fig. 3 and Table 2).

These findings are confirmed when TAMSAT is used as reference data. The Taylor diagrams (Figs. S6a-c) reveal many of the same characteristics as for the CHIRPS dataset (see Figs. 5a-c). A notable difference, however, is that regardless of the source of the boundary forcing the highest correlations are somewhat lower in the areas with two rainy seasons compared to CHIRPS. This is also revealed in the corresponding histograms, with narrower distributions with the highest values cut

off for the area with two rainy seasons for TAMSAT (Figs. S6d-f) compared to CHIRPS (see Fig. 5d-f). The corresponding medians with values of 0.52 for MPI-ESM, 0.17 for HadGEM and 0.23 for NorESM (Table S1) are somewhat lower than for CHIRPS. For the centred RMS deviations, the values of the medians for two rainy seasons are lowest for MPI-ESM with 1.02 and markedly higher for HadGEM with1.53 and NorESM with 1.61, respectively (Table S1). Hence, also in this case, the values of the medians confirm that RegCM is clearly best at simulating the seasonal variation of rainfall in East Africa, especially in the areas with two rainy seasons, when the boundary forcing originates from MPI-ESM.

The effects of the choice of the driving GCM on the simulation of the seasonal variation of rainfall in East Africa by RegCM are confirmed by the two other RCMs, showing a very similar behaviour (Figs. S7, S8). When the boundary forcing originates from MPI-ESM, RegCM is better at simulating the seasonal variation of rainfall in the areas with two dominant rainy seasons than CCLM and more so REMO, with values of the median of 0.56 for the correlations compared to 0.47 for CCLM and 0.38 for REMO and values of 0.92 compared to 1.03 for CCLM and 1.04 for REMO (Table 2).

3.3.2 Characteristics of rainy seasons

The difficulty of realistically simulating the seasonal variation of rainfall in the areas with two dominant rainy seasons when the boundary forcing originated from HadGEM and NorESM is reflected in the characteristics of the rainy seasons. In both cases the simulations are characterized by extensive areas with a different dominant rainy season where the observations are characterized by two dominant rainy seasons, typically with one dominant rainy season instead (e.g., Figs. 6a, 8a). Over the northern part of the Horn of Africa, however, the seasonal variation of rainfall is neither dominated by one nor two rainy seasons in the simulation driven by HadGEM (e.g., Fig 6a). Subsequently, these two simulations reveal diminished areas with two dominant rainy seasons, i.e., the triangle encompassing parts of Ethiopia, Kenya and Somalia, parts of western Kenya and southern Uganda in both cases, with a larger area over southern Uganda for HadGEM (e.g., Fig. 6a) and a notably larger area encompassing neighbouring parts of Ethiopia, Kenya and Somalia for NorESM (e.g., Fig. 8a). When the boundary forcing originated from MPI-ESM, the simulation represents the areas with two dominant rainy seasons very well, except for the coastal area of southern Somalia with one dominant rainy season (e.g., Fig. 7a).

For the simulation forced with MPI-ESM the characteristics of the rainy seasons (Fig. 7) are very similar to the simulation driven by ERA-Interim (see Fig. 4), with some of the regional deviations from the observations being more pronounced. For one rainy season, for instance, the onset is clearly earlier in the entire area south of the equator (Fig. 7a), leading to a longer rainy season over most of this area (Fig. 7c). Similarly, the onset of the second of two rainy seasons is earlier over the entire area except for southern Uganda (Fig. 7g), resulting in a notably extended rainy over the Horn of Africa by three to five weeks (Fig. 7i). The simulation forced with HadGEM shows similar tendencies in the regions where the dominant rainy seasons correspond to the observations with somewhat stronger deviations in some cases (Fig. 6). For one rainy season, for instance, the cessation is about four to six weeks earlier in northwestern Tanzania (Fig. 6b). The onset of the first of two rainy seasons, on the other hand, is delayed by about five to seven weeks in the area encompassing neighbouring parts of Ethiopia, Kenya and Somalia (Fig. 6d) leading to a markedly shorter rainy season in this region (Fig. 6f). The overall tendency and many of the regional details are also found in the simulation forced with NorESM (Fig. 8). In the case of two rainy seasons, the deviations from the observations become more obvious in the region including the neighbouring parts of Ethiopia, Kenya and Somalia (Figs. 8d-i) as it is larger than for HadGEM (Figs. 6d-i).

Using the TAMSAT dataset as reference reveals IDENTICAL effects of the choice of the driving GCM on the characteristics of the rainy seasons in East Africa simulated by RegCM, illustrated by very similar deviations from the observations, regarding both the geographical distributions and the magnitudes (Figs. S9-S11). For the first of two rainy seasons, however, using TAMSAT as reference data enhances the delay in the onset of the rainy season by up to several weeks (Figs. S9d, S10d, S11d) and, thus, the shortening of the rainy season by up to several weeks over most of the area (Figs. S9f, S10f, S11f).

The two other RCMs, CCLM and REMO, show corresponding effects of the choice of the driving GCM on the characteristics of the rainy seasons in East Africa (Figs. S12-S17), with some specific differences between the RCMs. CCLM, for instance, is much better at representing the dominance of two rainy seasons over Somalia when driven by HadGEM (e.g., Fig. S12d). For one rainy season, the three simulations with CCLM are characterised by a much earlier onset, later cessation and longer duration of the rainy season over the Ethiopian highlands (Figs. S12a-c, S13a-c, S14a-c) consistent with the simulation forced with ERA-Interim (see Fig. S4). REMO is considerably worse at representing the dominance of two rainy seasons over the Horn of Africa in

both the simulations forced with HadGEM (e.g., Fig. S15a) and NorESM (e.g., Fig. S17a).

4. Discussion

4.1 Errors induced by the driving GCMs

The timing of the two rainy seasons in East Africa is mainly determined by the migration of the Intertropical Convergence Zone into the local summer hemisphere governing the regions with large-scale atmospheric convergence and divergence and the reversals of the low-level atmospheric circulation associated with the East African monsoon system transporting moisture from the Indian Ocean into East Africa (e.g., Funk et al. 2016). During boreal spring and summer, the south-easterly flow associated with the rapid northward shift of the Somali Jet initiates a south-easterly transport of moisture into East Africa resulting in a rapid increase in rainfall in boreal spring to form the long rains. When the Indian summer monsoon intensifies in late boreal summer, the Somali Jet strengthens and shifts eastward, reducing the inflow of moisture from the Indian Ocean and generating subsidence in parts of eastern Kenya, southern Ethiopia and Somalia. When the Indian summer monsoon recedes in boreal fall, the reversing Indian trades bring moisture to feed the East African short rains.

Rainfall in East Africa is also affected by the Walker Circulation, particularly the Indian Ocean branch of the circulation (e.g., Zhao and Cook 2021; Palmer et al. 2023a). The Indian Ocean Walker Circulation (IOWC) governs the large-scale flow in East Africa in late boreal fall with subsidence over East Africa and an easterly low-level flow along the equator across the Indian Ocean into East Africa (e.g., Nicholson 2017). The Walker Circulation is strongly affected by the ENSO phenomenon, redistributing the areas with large-scale convergence and divergence across the tropical Indo-Pacific basins, with increased subsidence over East Africa during La Niña events and decreased subsidence over East Africa during El Niño events (e.g., Funk et al. 2023). The IOWC is also strongly affected by the IOD describing the oscillation of the SSTs between the western and the eastern part of the Indian Ocean (e.g., Palmer et al. 2023a). In its negative phase with relatively cold SSTs in the western Indian Ocean the IOD strengthens the Indian Ocean branch of the Walker Circulation with increased subsidence over East Africa and in its positive phase with rather warm SSTs the IOD weakens this branch of the Walker circulation with decreased subsidence and increased atmospheric convection in the region. As a result, rainfall in East Africa is reduced in late boreal fall during the negative phase of the IOD and increased during the positive phase (Roy and Troccoli 2024).

Thus, the realistic simulation of the seasonal variation of rainfall in East Africa in the RCMs crucially depends on the realistic representation of a complex set of related atmospheric and oceanic factors. Considering simulations from numerous GCMs from both CMIP5 and CMIP6, Schwarzwald et al. (2023) analysed how biases in these governing factors contributed to the biases in the representation of the long and short rains over the Greater Horn of Africa. They found that the key biases that had been identified in CMIP5 remained or even worsened in the later generation of GCMs contributing to CMIP6, including the tendency of long rains being too short and weak and short rains being too long and strong in the simulations. The wet biases in the short rains, for instance, were found to be linked to an erroneous zonal gradient of the SSTs in the Indian Ocean basin with too warm SSTs in the western part causing too deep convection. An erroneous timing of the seasonal cycle of the SSTs in the western Indian Ocean was coupled to biases in the timing of rainfall, but both shortcomings could have a common origin. King et al. (2020) identified errors in the representation of the IOWC as the key source of biases in the simulation of seasonal rainfall in Kenya in the GCMs contributing to CMIP5. The absence of the overturning cell of the IOWC at the equator during the short rains, for instance, was associated with a wet rainfall bias, while during the long rains the overestimated strength of the descending branch of the circulation over East Africa caused a dry rainfall bias.

Evaluating a very large number of models contributing to CMIP5, Dunning et al. (2017) showed that MPI-ESM simulated the two dominant rainy seasons over the Horn of Africa and in the central tropics very well, while HadGEM and even more so NorESM had difficulties to do so. The only other GCMs representing the onset and cessation of the rainy seasons over the Horn of Africa as realistically as MPI-ESM were CSIRO-Mk3 and IPSL-CM5A-MR.

4.2 Relation to the CORDEX simulations

The homogeneity of the simulations from the CORDEX-CORE experiment allows for a coordinated use of the climate projections for impact studies, which stands in contrast to the earlier simulations in the CORDEX program. Despite their inhomogeneity, several CORDEX ensemble studies are highly relevant in the context of our study. Nikulin et al. (2012), for instance, included nine of the RCMs from the CORDEX initiative to analyse the precipitation climatology in Africa as simulated by the RCMs when forced with ERA-Interim. The authors concluded that, overall, all RCMs simulated the seasonal mean and the annual cycle of precipitation quite realistically, but that some of the RCMs had significant biases in particular regions or seasons. Karypidou et al. (2023) focused on

the three RCMs that had been run with the largest number of driving GCMs from the CORDEX ensemble to assess the impact of the lateral boundary forcing on the simulation of the monthly precipitation climatology in southern Africa. The authors found that during the beginning of the rainy season the impact of the driving GCMs was smaller compared to the core of the rainy season, reflecting the different regional processes governing the seasonal variation of precipitation, e.g., the dominant role of the large-scale circulation, in the later stage of the rainy season.

4.3 Relation to the new CORDEX-CORE simulations

The regional climate simulations considered here have been performed with older versions of the RCMs and have been forced with atmospheric boundary conditions from GCMs that have been part of CMIP5. Currently the next phase of the CORDEX-CORE experiment is running and a new set of regional climate simulations for Africa will eventually become available, again with three RCMs and three GCMs selected from CMIP6 (CORDEX 2026). However, the older regional climate simulations are part of the Worldwide C3S CORDEX Grand Ensemble (e.g., Diez-Serra et al. 2022), contributing to the IPCC WGI interactive atlas (Gutiérrez et al. 2021) and being distributed via the Copernicus Climate Change Service (2026a). The regional climate simulations from the first CORDEX-CORE experiment for Africa have been used as input for various applications describing the role of climate change on different sectors across Africa (e.g., Copernicus Climate Change Service 2026b) and have been the basis for scientific publications on climate change impacts in Africa (e.g., Fotso-Nguemo et al. 2023; Soares et al. 2024). Hence, the evaluation remains highly relevant. In addition, the climate scenario simulations have been provided for two emission scenarios, i.e., the RCP2.6 and the RCP8.5 scenario (e.g., Van Vuuren et al. 2011), spanning the range between a scenario with a weak radiative forcing and a scenario with a very strong radiative forcing. In the new CORDEX-CORE experiment only one climate scenario is included, i.e., the SSP3-7.0 scenario (e.g., O'Neill et al. 2016) with a strong radiative forcing and, thus, does not allow for assessing the climatic changes associated a global warming of 2 °C associated with a much weaker radiative forcing.

Our work will also be important in guiding the evaluation of the new simulations as they become available. In these new simulations, updated versions of the RCMs considered here, i.e., the fifth-generation version of RegCM (Giorgi et al. 2023) and the REMO version from 2020 (Pietikäinen et al. 2025) are used, complemented by the HadREM3-GA7-05 RCM (Tucker et al. 2022). Also updated versions of the MPI-ESM (Mauritsen et al. 2019) and NorESM (Seland et al. 2020) GCMs contributing to CMIP6 are considered, and EC-Earth-Veg (Döscher et al. 2022) is the third GCM

providing atmospheric boundary conditions. Since, however, the GCMs from CMIP6 in general have not become better at representing the seasonal variation of rainfall in East Africa (Schwarzwald et al. 2023), it will be necessary to also evaluate the seasonal variation of rainfall in this region in the new set of regional climate simulations to be able to identify the most viable climate scenarios.

4.4 Definitions of the rainy seasons

The method used to determine the characteristics of the rainy seasons is based on the method described in Dunning et al. (2016), with the difference that the onset and cessation dates were not computed for individual years (and then averaged) but based on the climatological annual cycle of daily precipitation at each location. The latter reduced the uncertainty of the estimates, given strong interannual variations in the onset and cessation dates of the rainy seasons but did not affect the main features of the characteristics of the rainy seasons (not shown here). The updated method allowed for an objective determination of the characteristics of the rainy seasons across entire East Africa comprising different climate zones as well as across observational data and data from climate simulations. When applying their method to several observational datasets of daily precipitation across Africa, Dunning et al. (2016) found the same differentiation of regions with one and two dominant rainy seasons and very similar geographical distributions of the onset and cessation dates of the rainy seasons in East Africa as described here.

There are various alternative ways to define the onset and cessation dates of rainy seasons. Omay et al. (2023), for instance, distinguished between the four standard climatological seasons when defining criteria for the onset and the cessation dates in the northern part of Eastern Africa. The authors defined the onset date by a threshold of the rainfall total (20 mm over 5 days with at least 3 wet days) without a dry spell exceeding 7 days during the next 21 days. The cessation date was defined by the fraction of evapotranspiration, with 10 days of rainfall below half of the evapotranspiration. When analysing the length of the growing season in the Kenyan highlands, Ngetich et al. (2014) based their definition of the onset dates of the long and short rain seasons as the first wet day (at least 0.85 mm of rainfall) with at least 25 mm of accumulated rainfall in what they considered a semi-humid region and 30 mm in a humid region during a maximum of 3 and 5 successive days, respectively. The authors used the soil water balance for defining the cessation dates, i.e., the date on which the water stress coefficient exceeded a value of 0.4. These types of definitions of the onset and cessation of the rainy seasons are very specific to the local context and, thus, typically not applicable for other regions, in particular not for entire East Africa. Even for the regions, for

514 which these definitions have been developed, they are not really suitable for climate simulations
515 because of the different scales (grid point vs. point observation) and because of biases in the
516 simulation of the relevant aspects of the hydrological cycle.

517 ### 4.5 Uncertainty of the observations

518 To estimate the uncertainty related to the choice of a specific observational dataset as reference (e.g.,
519 Salami et al. 2025), we considered the CHIRPS as the main reference data being presented in the
520 main analysis and TAMSAT as the additional reference data, with analyses in the supplementary
521 material. As discussed in Sect. 2.1, both datasets are of equally high quality, including the statistics
522 of daily precipitation in East Africa, and choosing one of the datasets over the other is purely
523 subjective. The evaluations presented here have shown that the overall quality of the seasonal
524 variation of rainfall in East Africa in the simulations as measured by the Taylor diagrams and the
525 regional deviations in the characteristics of the rainy seasons, both the geographical distributions and
526 the magnitudes, are very similar for the two observational datasets, meaning that the findings of our
527 study are robust.

528 ## 5. Summary and conclusions

529 In this study, we evaluated the extent to which the three RCMs (CCLM, RegCM and REMO)
530 contributing to the CORDEX-CORE experiment represent the seasonal variation of rainfall in East
531 Africa in accordance with observations of daily rainfall. This is an imperative step to determine the
532 suitability of the regional climate simulations with specific combinations of RCMs and driving GCMs
533 (HadGEM, MPI-ESM and NorESM) for assessing potential impacts of future climate change on
534 agriculture in the region based on the scenario simulations provided by these models.

535 The simulations forced with the ERA-Interim reanalyses illustrated that RegCM is best among
536 the three RCMs at representing the seasonal variation of rainfall in East Africa. This is particularly
537 the case for the phase of the climatological annual cycle of daily rainfall in the regions with two
538 dominant rainy seasons. RegCM is also slightly better than the two other RCMs at representing the
539 shape and magnitude of the climatological annual cycle of rainfall. As for the characteristics of the
540 rainy seasons (onset, cessation and length) each of the three RCMs shows specific geographical
541 distributions of the deviations from the observations, with comparable magnitudes of the regional
542 differences for the three RCMs.

543 The simulations forced with the boundary conditions originating from the three GCMs
544 indicated that only the simulations with the boundary conditions from MPI-ESM represent the
545 seasonal variation of rainfall in East Africa realistically. When forced with HadGEM or NorESM, the
546 RCMs have deficiencies in capturing the climatological annual cycle of rainfall in the regions with
547 two dominant rainy seasons, typically simulating one dominant rainy season instead. The choice of
548 the GCM for the boundary forcing has a minor effect on the regional deviations from the observations
549 for the characteristics of the rainy seasons, for the simulations driven by HadGEM or NorESM,
550 however, confined to much smaller areas in the case of two dominant rainy seasons.

551 These results support our hypothesis that the representation of the large-scale atmospheric flow
552 around Africa and of remote forcings such as the IOD and ENSO (e.g., Nicholson 2017; Palmer et al.
553 2023a) in the GCMs providing the boundary forcing has a strong influence on the simulation of the
554 seasonal variation of rainfall in East Africa by the three RCMs. Given the complex nature of the
555 processes governing the occurrence of rainfall associated with the two rainy seasons over the Horn
556 of Africa and in the central tropics, there are various potential sources for errors introduced by the
557 GCMs (e.g., Schwarzwald et al. 2023). Investigating these sources of the specific errors in the GCMs
558 in detail would be a comprehensive study and, therefore, was not pursued here.

559 Our findings have important implications for using the climate scenarios from the CORDEX-
560 CORE experiment for the assessment of the potential impacts of future climate change in East Africa
561 on sectors that are closely connected to the occurrence of rainfall during the rainy seasons. We
562 therefore recommend using only regional climate simulations forced with MPI-ESM for impact
563 assessments for regions with two dominant rainy seasons or East Africa as a whole. When the focus
564 is on regions with one dominant rainy season, the choice of the driving GCM among the three is not
565 crucial. Although RegCM best simulates the seasonal variation of rainfall in East Africa overall, the
566 quality of CCLM and REMO (except for southernmost Somalia) is good enough to recommend using
567 simulations from all three RCMs for impact assessments, given that the atmospheric boundary
568 conditions from the driving GCM are sufficiently realistic. As each of the three RCMs is characterized
569 by specific geographical distributions of the deviations from observations for the characteristics of
570 the rainy seasons in East Africa, this allows for taking the uncertainty related to the specific RCMs
571 into account in impact assessments and, thus, in the design of measures to adapt to the adverse effects
572 of climate change.

573 Our findings also serve as a point of departure for evaluating the new set of regional climate

simulations in the COREX-CORE experiment for Africa, which are planned or currently under way (CORDEX 2026). In the new set of simulations, again, three RCMs are used to downscale historical and scenario simulations from three different GCMs. In the new simulations, updated versions of two of the RCMs considered here, i.e., the fifth-generation version of RegCM and the REMO version from 2020 are used and updated versions of two of the GCMs used here (MPI-ESM and NorESM) are considered. This allows for evaluating the progress that has been made in simulating the seasonal variation of rainfall in East Africa by the RCMs over the last five to seven years, either due to improvements of the governing processes in the RCMs or due to more realistic representations of the large-scale atmospheric circulation and the state of the oceans controlling the seasonal climate variability in East Africa in the GCMs.

Acknowledgements

Thanks to the Climate Hazards Center at UC Santa Barbara (CHIRPS) and the University of Reading (TAMSAT) for providing the observational precipitation data as well as the Climate Service Center Germany (GERICS), the Abdus Salam International Centre for Theoretical Physics (ICTP) and the Karlsruhe Institute of Technology (KIT) for providing the data from the CORDEX-CORE experiments for Africa. Thanks also to Nikolaos Alexandridis for fruitful discussions during this work. Access to the computer facilities at the European Centre for Medium-Range Weather Forecasts (ECMWF), where the analysis was done, is granted through the special project on 'The role of forest management and land-use changes for anthropogenic climate forcing'. The research presented in this paper is a contribution to the Swedish Strategic Research Area 'Modelling the Regional and Global Earth System (MERGE)' and to the Swedish Strategic Research Area 'Biodiversity and ecosystem services in a changing climate (BECC)'.

Competing interests The authors declare that they have no competing interests.

Funding statement Swedish Research Council project 'Towards sustainable maize production in East Africa: Cropping system resilience under climate change' with grant number 2018-05843; European Union's Horizon 2020 project 'Upscaling the benefits of Push-Pull technology for sustainable agricultural intensification in East Africa (UPSCALE)' with grant number 861998 for both Wilhelm May and Yann Clough; Swedish Strategic Research Area 'Modelling the regional and global earth system (MERGE)' for Wilhelm May; Swedish Strategic Research Area 'Biodiversity and ecosystem services in a changing climate (BECC)' for Yann Clough.

Authors' contributions Wilhelm May designed the study, performed the analyses and prepared the manuscript; Yann Clough contributed to the design of the study and the preparation of the manuscript and raised the project funding.

Data availability The observational datasets used in the study can be downloaded from the relevant sites, i.e., https://data.chc.ucsb.edu/products/CHIRPS-2.0/africa_daily/ for the CHIRPS dataset and https://data.tamsat.org.uk/data-download/rainfall/ for the TAMSAT dataset, respectively. The data from the CORDEX-CORE simulations can be downloaded from the respective ESGF nodes.

607 **Supplementary information** The supplementary information is provided in an additional file.

References

Ashfaq M, Cavazos T, Reboita MS, Torres-Alavez JE, Im E-S, Olusegun CF, Alves L, Key K, Adeniyi MO, Tall M, Sylla MB, Mehmood S, Zafar Q, Das S, Diallo I, Coppola E, Giorgi F (2021) Robust late twenty-first century shift in the regional monsoons in RegCM-CORDEX simulations. Clim Dyn 57:1463-1488. https://doi.org/10.1007/s00382-020-05306-2

Bentsen M, Bethke I, Debernard JB, Iversen T, Kirkevåg A, Seland Ø, Drange H, Roelandt C, Seierstad IA, Hoose C, Kristjánsson JE (2013) The Norwegian Earth System Model, NorESM1-M – Part 1: Description and basic evaluation of the physical climate. Geosci Model Dev 6:687-720. https://doi.org/10.5194/gmd-6-687-2013

Challinor AJ, Watson J, Lobell DB, Howden SM, Smith DR, Chhetri N (2014) A meta-analysis of crop yield under climate change and adaptation. Nat Clim Change 4:287-291. https://doi.org/10.1038/NCLIMATE2153

Coppola E, Raffaele F, Giorgi F, Giuliani G, Xuejie G, Ciarlo JM, Sines TR, Torres-Alavez JA, Das S, di Sante F, Pichelli E, Glazer R, Müller SK, Omar SA, Ashfaq M, Bukovsky M, Im E-S, Jacob D, Teichmann C, Remedio A, Remke T, Kriegsmann A, Bülow K, Weber T, Buntemeyer L, Sieck K, Rechid D (2021) Climate hazard indices projections based on CORDEX-CORE, CMIP5, and CMIP6 ensembles. Clim Dyn 57:1293-1383. https://doi.org/10.1007/s00382-021-05640-z

Copernicus Climate Change Service (2026a) CORDEX regional climate model data on single levels. https://cds.climate.copernicus.eu/datasets/projections-cordex-domains-single-levels?tab=overview. Assessed 28 September 2026

Copernicus Climate Change Service (2026b) Copernicus Africa Overview. https://climate.copernicus.eu/taxonomy/term/132. Assessed 28 October 2026

CORDEX (2026) CORDEX CMIP6 downscaling plans. https://wcrp-cordex.github.io/simulation-status/CMIP6_downscaling_plans.html. Assessed 26 September 2026

Dee DP, Uppala SM, Simmons AJ, Berrisford P, Poli P, Kobayashi S, Andrae U, Balmaseda MA, Balsamo G, Bauer P, Bechtold P, Beljaars ACM, van de Berg L, Bidlot J, Bormann N, Delsol C, Dragani R, Fuentes M, Geer AJ, Haimberger L, Healy SB, Hersbach H, Hólm EV, Isaksen L, Kållberg P, Köhler M, Matricardi M, McNally AP, Monge-Sanz BM, Morcrette J-J, Park B-K, Peubey C, de Rosnay P, Tavolato C, Thépaut J-N, Vitart (2011) The ERA-Interim reanalysis: configuration and performance of the data assimilation systems. Q J R Meteorol Soc 137:553-597. https://doi.org/10.1002/qj.828

Diez-Sierra J, Iturbide M, Gutiérrez JM, Fernández J, Milovac J, Cofiño AS, Cimadevilla E, Nikulin G, Levavasseur G, Kjellström E, Bülow K, Horányi A, Brookshaw A, García-Díez M, Pérez A, Baño-Medina J, Ahrens B, Alias A, Ashfaq M, Bukovsky M, Buonomo E, Caluwaerts S, Chou SC, Christensen OB, Ciarlò JM, Coppola E, Corre L, Demory M-E, Djurdjevic V, Evans JP, Fealy R, Feldmann H, Jacob D, Jayanarayanan S, Katzfey J, Keuler K, Kittel C, Kurnaz ML, Laprise R, Lionello P, McGinnis S, Mercogliano P, Nabat P, Önol B, Ozturk

T, Panitz H-J, Paquin D, Pieczka I, Raffaele F, Remedio AR, Scinocca J, Sevault F, Somot S, Steger C, Tangang F, Teichmann C, Termonia P, Thatcher M, Torma C, van Meijgaard E, Vautard R, Warrach-Sagi K, Winger K, Zittis G (2022) The worldwide C3S CORDEX Grand Ensemble: A major contribution to assess regional climate change in the IPCC AR6 Atlas. Bull Am Meteorol Soc 103:E2804-E2826. https://doi.org/10.1175/BAMS-D-22-0111.1

Dinku T, Funk C, Peterson P, Maidment R, Tadesse T, Gadain H, Ceccato P (2018) Validation of the CHIRPS satellite rainfall estimates over eastern Africa. Q J R Meteorol Soc 144:292-312. https://doi.org/10.1002/qj.3244

Döscher R, Acosta M, Alessandri A, Anthoni P, Arsouze T, Bergman T, Bernardello R, Boussetta S, Caron L-P, Carver G, Castrillo M, Catalano F, Civijanovic I, Davini P, Dekker E, Doblas-Reyes FJ, Docquier D, Echevarria P, Fladrich U, Fuentes-Franco R, Gröger M, von Hardenberg J, Hieronymus J, Karami MP, Keskinen J-P, Koenigk T, Makkonen R, Massonnet F, Ménégoz M, Miller PA, Moreno-Chamarro E, Nieradzik L, van Noije T, Nolan P, O'Donnell D, Ollinaho P, van den Oord G, Ortega P, Prims OT, Ramos A, Reerink T, Rousset C, Ruprich-Robert Y, le Sager P, Schmith T, Schrödner R, Serva F, Sicardi V, Madsen MS, Smith B, Tian T, Tourigny E, Uotila P, Vancoppenolle M, Wang S, Wårlind D, Willén U, Wyser K, Yang S, Yepes-Arbós X, Zhang Q (2022) The EC-Earth3 Earth system model for the Coupled Model Intercomparison Project 6. Geosci Model Dev 15:2973-3020. https://doi.org/10.5194/gmd-15-2973-2022

Dosio A, Pinto I, Lennard C, Sylla MB, Jack C, Nikulin G (2021) What can we know about recent past precipitation over Africa? Daily characteristics of African precipitation from a large ensemble of observational products for model evaluation. Earth Space Sci 8:e2020EA001466. https://doi.org/10.1029/2020EA001466

Dunning CM, Black E, Allan RP (2016) The onset and cessation of seasonal rainfall over Africa. J Geophys Res 121:11405-11424. https://doi.org/10.1002/2016JD025428

Dunning CM, Allan RP, Black E (2017) Identification of deficiencies in seasonal rainfall simulated by CMIP5 climate models. Environ Res Lett 12:14001. https://doi.org/10.1088/1748-9326/aa869e

Ericksen PJ, Ingram JSI, Liverman DM (2009) Food security and global environmental change: emerging challenges. Environ Sci Policy 12:373-377. https://doi.org/10.1016/j.agee.2020.107199

Fotso-Nguemo TC, Weber T, Diedhiou A, Chouto S, Vondou DA, Rechid D, Jacob D (2023) Projected impact of increased global warming on heat stress and exposed population over Africa. Earth's Future 11:e2022EF003268. https://doi.org/10.1029/2022EF003268

Funk C, Peterson P, Landsfeld M, Pedreros D, Verdin J, Shukla S, Husak G, Rowland J, Harrison L, Hoell A, Michaelsen J (2015) The climate hazards infrared precipitation with stations – a new environmental record for monitoring extremes. Sci Data 2:150066. https://doi.org/10.1038/sdata.2015.66

Funk C, Hoell A, Shukla S, Husak G, Michaelsen J (2016) The East African monsoon system: Seasonal climatologies and recent variations. In The Monsoons and Climate Change. Observations and Modeling [De Carvalho LMV, Jones C (eds)]. Springer, Heidelberg, Germany, pp 163-185

Funk C, Fink AH, Harrison L, Segele Z, Endris HS, Galu G, Korecha D, Nicholson S (2023) Frequent but predictable

droughts in East Africa driven by a Walker Circulation intensification. Earths Future 11:e2022EF003454. https://doi.org/10.1029/2022EF003454

Gebrechorkos SH, Hülsmann S, Bernhofer C (2018) Evaluation of multiple climate data sources for managing environmental resources in East Africa. Hydrol Earth Syst Sci 22:4547-4564. https://doi.org/10.5194/hess-22-4547-2018

Giorgetta MA, Jungclaus J, Reick CH, Legutke S, Bader J, Böttinger M, Brovkin V, Crueger T, Esch M, Fieg K, Glushak K, Gayler V, Haak H, Hollweg H-D, Ilyina T, Kinne S, Kornblueh L, Matei D, Mauritsen T, Mikolajewicz U, Mueller W, Notz D, Pithan F, Raddatz T, Rast S, Redler R, Roeckner E, Schmidt H, Schnur R, Segschneider J, Six KD, Stockhause M, Timmreck C, Wegner J, Widmann H, Wieners K-H, Claussen M, Marotzke J, Stevens S (2013) Climate and carbon cycle changes from 1850 to 2100 in MPI-ESM simulations for the Coupled Model Intercomparison Project Phase 5. J Adv Model Earth Syst 5:572-597. https://doi.org/10.1002/jame.20038

Giorgi F, Jones C, Asrar GR (2009) Addressing climate information needs at the regional level: the CORDEX framework. WMO Bull 58:175-183

Giorgi F, Coppola E, Solmon F, Mariotti L, Sylla MB, Bi X, Elguindi N, Diro GT, Nair V, Giuliani G, Turuncoglu UU, Cozzini S, Güttler I, O'Brien TA, Tawfik AB, Shalaby A, Zakey AS, Steiner AL, Stordal F, Sloan LC, Brankovic C (2012) RegCM4: model description and preliminary tests over multiple CORDEX domains. Clim Res 52:7-29. https://doi.org/10.3354/cr01018

Giorgi F, Gutowski Jr WJ (2015) Regional dynamical downscaling and the CORDEX Initiative. Annu Rev Environ Resour 40:467-490. https://doi.org/10.1146/annurev-environ-102014-021217

Giorgi F (2019) Thirty years of regional climate modeling: Where are we and where are we going next? J Geophys Res 124:5696-5723. https://doi.org/10.1029/2018JD030094

Giorgi F, Coppola E, Teichmann C, Jacob D (2021) Editorial for the CORDEX-CORE Experiment I Special Issue. Clim Dyn 57:1265-1268. https://doi.org/10.1007/s00382-021-05902-w

Giorgi F, Coppola E, Jacob D, Teichmann C, Omar SA, Ashfaq M, Ban N, Bülow K, Bukovsky M, Buntemeyer L, Cavazos T, Ciarlo J, da Rocha RP, Das S, di Sante F, Evans JP, Gao X, Giuliani G, Glazer RH, Hoffmann P, Im E-S, Langendijk G, Lierhammer L, Llopart M, Mueller S, Luna-Nino R, Nogherotto R, Pichelli P, Raffaele F, Reboita M, Rechid D, Remedio A, Remke T, Sawadogo W, Sieck K, Torres-Alavez JA, Weber T (2022) The CORDEX-CORE EXP-I initiative: Description and highlight results from the initial analysis. Bull Am Meteorol Soc 103:E293-E310. https://doi.org/10.1175/BAMS-D-21-0119.1

Giorgi F, Coppola E, Giuliani G, Ciarlo` JM, Pichelli E, Nogherotto R, Raffaele F, Malguzzi P, Davolio S, Drofa O (2023) The Fifth Generation Regional Climate Modeling System, RegCM5: Description and illustrative examples at parameterized convection and convection-permitting resolutions. J Geophys Res 128:e2022JD038199.

Gutiérrez JM, Jones RG, Narisma GT, Alves LM, Amjad M, Gorodetskaya IV, Grose M, Klutse NAB, Krakovska S, Li J, Martínez-Castro D, Mearns LO, Mernild SH, Ngo-Duc T, van den Hurk B, Yoon J-H (2021): Atlas. In

Climate Change 2021: The Physical Science Basis. Contribution of Working Group I to the Sixth Assessment Report of the Intergovernmental Panel on Climate Change [Masson-Delmotte V, Zhai P, Pirani A, Connors SL, Péan C, Berger S, Caud N, Chen Y, Goldfarb L, Gomis MI, Huang M, Leitzell K, Lonnoy E, Matthews JBR, Maycock TK, Waterfield T, Yelekçi O, Yu R, Zhou B (eds)]. Cambridge University Press, Cambridge, United Kingdom and New York, NY, USA, pp 1927-2058

Gutowski Jr WJ, Giorgi F, Timbal B, Frigon A, Jacob D, Kang H-S, Raghavan K, Lee B, Lennard C, Nikulin G, O'Rourke E, Rixen M, Solman S, Stephenson T, Tangang F (2016) WCRP COordinated Regional Downscaling EXperiment (CORDEX): a diagnostic MIP for CMIP6. Geosci Model Dev 9:4087-4095. https://doi.org/10.5194/gmd-9-4087-2016

IPCC (2021) Summary for Policymakers. In: Climate Change 2021: The Physical Science Basis. Contribution of Working Group I to the Sixth Assessment Report of the Intergovernmental Panel on Climate Change [Masson-Delmotte V, Zhai P, Pirani A, Connors SL, Péan C, Berger S, Caud N, Chen Y, Goldfarb L, Gomis MI, Huang M, Leitzell K, Lonnoy E, Matthews JBR, Maycock TK, Waterfield T, Yelekçi O, Yu R, Zhou B (eds)]. Cambridge University Press, Cambridge, United Kingdom and New York, NY, USA, pp 31

Jacob D, Elizalde A, Haensler A, Hagemann S, Kumar P, Podzun R, Rechid D, Remedio AR, Saeed F, Sieck K, Teichmann C, Wilhelm C (2012) Assessing the transferability of the regional climate model REMO to different coordinated regional climate downscaling experiment (CORDEX) regions. Atmosphere 3:181-199. https://doi.org/10.3390/atmos3010181

Jones C, Giorgi F, Asrar G (2011) The Coordinated Regional Downscaling Experiment: CORDEX, an international downscaling link to CMIP5. CLIVAR Exch 16:34-40

Jones CD, Hughes JK, Bellouin N, Hardiman SC, Jones GS, Knight J, Liddicoat S, O'Connor FM, Andres RJ, Bell C, Boo K-O, Bozzo A, Butchart N, Cadule P, Corbin KD, Doutriaux-Boucher M, Friedlingstein P, Gornall J, Gray L, Halloran PR, Hurtt G, Ingram WJ, Lamarque J-F, Law RM, Meinshausen M, Osprey S, Palin EJ, Parsons Chini L, Raddatz T, Sanderson MG, Sellar AA, Schurer A, Valdes P, Wood N, Woodward S, Yoshioka M, Zerroukat M (2011) The HadGEM2-ES implementation of CMIP5 centennial simulations. Geosci Model Dev 4:543-570. https://doi.org/10.5194/gmd-4-543-2011

Karypidou MC, Sobolowski SP, Sangelantoni L, Nikulin G, Katragkou E (2023) The impact of lateral boundary forcing in the CORDEX-Africa ensemble over southern Africa. Geosci Model Dev 16:1887-1908. https://doi.org/10.5194/gmd-16-1887-2023

King JA, Washington R, Engelstaedter S (2020) Representation of the Indian Ocean Walker circulation in climate models and links to Kenyan rainfall. Int J Climatol 41:616-643. https://doi.org/10.1002/joc.6714

Maidment R, Grimes D, Allan RP, Tarnavsky E, Stringer M, Hewison T, Roebeling R, Black E (2014) The 30 year TAMSAT African Rainfall Climatology And Time series (TARCAT) data set. J Geophys Res 119:10619-10644. https://doi.org/10.1002/2014JD021927

Maidment R, Grimes D, Black E, Tarnavsky E, Young M, Greatrex H, Allan RP, Stein T, Nkonde E, Senkunda S, Alcántara EMU (2017) A new, long-term daily satellite-based rainfall dataset for operational monitoring in

Africa. Sci Data 4:170063. https://doi.org/10.1038/sdata.2017.63

Mauritsen T, Bader J, Becker T, Behrens J, Bittner M, Brokopf R, Brovkin V, Claussen M, Crueger T, Esch M, Fast I, Fiedler S, Fläschner D, Gayler V, Giorgetta M, Goll DS, Haak H, Hagemann S, Hedemann C, Hohenegger C, Ilyina T, Jahns T, Jimenéz-de-la-Cuesta D, Jungclaus J, Kleinen T, Kloster S, Kracher D, Kinne S, Kleberg D, Lasslop G, Kornblueh L, Marotzke J, Matei D, Meraner K, Mikolajewicz U, Modali K, Möbis B, Müller WA, Nabel JEMS, Nam CCW, Notz D, Nyawira S-S, Paulsen H, Peters K, Pincus R, Pohlmann H, Pongratz J, Popp M, Raddatz TJ, Rast S, Redler R, Reick CH, Rohrschneider T, Schemann V, Schmidt H, Schnur R, Schulzweida U, Six KD, Stein L, Stemmler I, Stevens B, von Storch J-S, Tian F, Voigt A, Vrese P, Wieners K-H, Wilkenskjeld S, Winkler A, Roeckner E (2019) Developments in the MPI-M Earth System Model version 1.2 (MPI-ESM1.2) and its response to increasing CO_2. J Adv Model Earth Syst 11:998-1038. https://doi.org/10.1029/2018MS001400

May W, Shea DJ, Madden RA (1992) The annual variation of surface temperatures over the world. NCAR Technical Note NCAR/TN-372+STR, Boulder, CO, USA, pp 134

Nakawuka P, Langan S, Schmitter P, Barron J (2018) A review of trends, constraints and opportunities of smallholder irrigation in East Africa. Glob Food Secur 17:196-212. https://doi.org/10.1016/j.gfs.2017.10.003

Ngetich KF, Mucheru-Munaa M, Mugwea JN, Shisanya CA, Diels J, Mugendi DN (2014) Length of growing season, rainfall temporal distribution, onset and cessation dates in the Kenyan highlands. Agric For Meteorol 188:24-32. https://doi.org/10.1016/j.agrfomet.2013.12.011

Nicholson SE (2017) Climate and climatic variability of rainfall over eastern Africa. Rev Geophys 55:590-635. https://doi.org/10.1002/2016RG000544

Nikulin G, Jones C, Giorgi F, Asrar G, Büchner M, Cerezo-Mota R, Christensen OB, Déqué M, Fernandez J, Hänsler A, van Mejgaard E, Samuelsson P, Sylla MB, Sushama L (2012) Precipitation climatology in an ensemble of CORDEX-Africa regional climate simulations. J Clim 25:6057-6078. https://doi.org/10.1175/JCLI-D-11-00375.1

Omay PO, Muthama NJ, Oludhe C, Kinama JM, Artan G, Atheru Z (2023) Changes and variability in rainfall onset, cessation, and length of rainy season in the IGAD region of Eastern Africa. Theor Appl Climatol 152:871-893. https://doi.org/10.1007/s00704-023-04433-0

O'Neill BC, Tebaldi C, van Vuuren DP, Eyring V, Friedlingstein P, Hurtt G, Knutti R, Kriegler E, Lamarque J-F, Lowe J, Meehl GA, Moss R, Riahi K, Sanderson BM (2016) The Scenario Model Intercomparison Project (ScenarioMIP) for CMIP6. Geosci Model Dev 9:3461-3482. https://doi.org/10.5194/gmd-9-3461-2016

Palmer PI, Wainwright CM, Dong B, Maidment RI, Wheeler KG, Gedney N, Hickman JE, Madani M, Folwell SS, Abdo G, Allan RP, Black ECL, Feng L, Gudoshava M, Haines K, Huntingford C, Kilavi M, Lunt MF, Shaaban A. Turner AG (2023a) Drivers and impacts of Eastern African rainfall variability. Nat Rev Earth Environ 4:254-270. https://doi.org/10.1038/s43017-023-00397-x

Palmer TE, McSweeney CF, Booth BBB, MDK, Davini P, Brunner L, Borchert L, Menary MB (2023b) Performance-

based sub-selection of CMIP6 models for impact assessments in Europe. Earth Syst Dynam 14:457-483. https://doi.org/10.5194/esd-14-457-2023

Pietikäinen J-P, Sieck K, Buntemeyer L, Frisius T, Nam C, Hoffmann P, Pop C, Rechid D, Jacob D (2025) REMO2020: a modernised modular regional climate model. Geosci Model Dev 18:7907-7949. https://doi.org/10.5194/gmd-18-7907-2025

Porkka M, Wang-Erlandsson L, Destouni G, Ekman AML, Rockström J, Gordon LJ (2021) Is wetter better? Exploring agriculturally-relevant rainfall characteristics over four decades in the Sahel. Environ Res Lett 15:035002. https://doi.org/10.1088/1748-9326/abdd57

Remedio AR, Teichmann C, Buntemeyer L, Sieck K, Weber T, Rechid D, Hoffmann P, Nam C, Kotova L, Jacob D (2019) Evaluation of new CORDEX simulations using an update Koppen-Trewartha climate classification. Atmosphere 10:726. https://doi.org/10.3390/atmos10110726

Roy I, Troccoli A (2024) Identifying important drivers of East African October to December rainfall season. Sci Tot Environ 914:169615. https://doi.org/10.1016/j.scitotenv.2023.169615

Rummukainen M (2016) Added value in regional climate modeling. WIREs Clim Change 7:145-159. https://doi.org/10.1002/wcc.378

Salami AA (2025) Rainfall variability and trends analyses in Nigeria using remotely sensed data and CMIP5 models. Earth Syst Environ 9:2837-2865. https://doi.org/10.1007/s41748-024-00556-0

Schwarzwald K, Goddard L, Seager R, Ting M, Marveille K (2023) Understanding CMIP6 biases in the representation of the Greater Horn of Africa long and short rains. Clim Dyn 61:1229-1255. https://doi.org/10.1007/s00382-022-06622-5

Seland Ø, Bentsen M, Olivié D, Toniazzo T, Gjermundsen A, Graff LS, Debernard JB, Gupta AK, He Y-C, Kirkevåg A, Schwinger J, Tjiputra J, Aas KS, Bethke I, Fan Y, Griesfeller J, Grini A, Guo C, Ilicak M, Karset IHH, Landgren O, Liakka J, Moseid KO, Nummelin A, Spensberger C, Tang H, Zhang Z, Heinze C, Iversen T, Schulz M (2020) Overview of the Norwegian Earth System Model (NorESM2) and key climate response of CMIP6 DECK, historical, and scenario simulations. Geosci Model Dev 13:6165-6200. https://doi.org/10.5194/gmd-13-6165-2020

Seneviratne SI, Zhang X, Adnan M, Badi W, Dereczynski C, Di Luca A, Ghosh S, Iskandar I, Kossin J, Lewis S, Otto F, Pinto I, Satoh M, Vicente-Serrano SM, Wehner M, Zhou,B (2021) Weather and Climate Extreme Events in a Changing Climate. In: Climate Change 2021: The Physical Science Basis. Contribution of Working Group I to the Sixth Assessment Report of the Intergovernmental Panel on Climate Change [Masson-Delmotte V, Zhai P, Pirani A, Connors SL, Péan C, Berger S, Caud N, Chen Y, Goldfarb L, Gomis MI, Huang M, Leitzell K, Lonnoy E, Matthews JBR, Maycock TK, Waterfield T, Yelekçi O, Yu R, Zhou B (eds)]. Cambridge University Press, Cambridge, United Kingdom and New York, NY, USA, pp 1513-1765

Soares PMM, Careto JAM, Lima DCA (2024) Future extreme and compound events in Angola: CORDEX-Africa regional climate modelling projections. Weather Clim Extr 45:100691.

https://doi.org/10.1016/j.wace.2024.100691

Sørland SL, Brogli R, Pothapakula PK, Russo E, van de Walle J, Ahrens B, Anders I, Bucchignani E, Davin EL, Demory M-E, Dosio A, Feldmann H, Früh B, Geyer B, Keuler K, Lee D, Li D, van Lipzig NPM, Min S-K, Panitz H-J, Rockel B, Schär C, Steger C, Thiery W (2021) COSMO-CLM regional climate simulations in the Coordinated Regional Climate Downscaling Experiment (CORDEX) framework: a review. Geosci Model Dev 14:5125-5154. https://doi.org/10.5194/gmd-14-5125-2021

Tarnavsky E, Grimes D, Maidment R, Black E, Allan R, Stringer M, Chadwick R, Kayitakire F (2014) Extension of the TAMSAT satellite-based rainfall monitoring over Africa and from 1983 to present. J Appl Meteorol Clim 53:2805-2822. https://doi.org/10.1175/JAMC-D-14-0016.1

Taylor, KE (2001) Summarizing multiple aspects of model performance in a single diagram. J Geophys Res 106:7183-7192. https://doi.org/10.1029/2000JD900719

Teichmann C, Jacob D, Remedio AR, Remke T, Buntemeyer L, Hoffmann P, Kriegsmann A, Lierhammer L, Bülow K, Weber T, Sieck K, Rechid D, Langendijk GS, Coppola E, Giorgi F, Ciarlo JM, Raffaele F, Giuliani G, Xuejie G, Sines TR, Torres-Alavez JA, Das S, Di Sante F, Pichelli E, Glazer R, Ashfaq M, Bukovsky M, Im E-S (2021) Assessing mean climate change signals in the global CORDEX-CORE ensemble. Clim Dyn 57:1269-1292. https://doi.org/10.1007/s00382-020-05494-x

Tucker SO, Kendon EJ, Bellouin N, Buonomo E, Johnson B, Murphy JM (2022) Evaluation of a new 12 km regional perturbed parameter ensemble over Europe. Clim Dyn 58:879-903. https://doi.org/10.1007/s00382-021-05941-3

Van Vuuren DP, Edmonds J, Kainuma M, Riahi K, Thomson A, Hibbard K, Hurtt GC, Kram T, Krey V, Lamarque J-F, Masui T, Meinshausen M, Nakicenovic N, Smith SJ, Rose SK (2011) The representative concentration pathways: an overview. Clim Change 109:5-31. https://doi.org/10.1007/s10584-011-0148-z

Zhao S, Cook KH (2021) Influence of Walker circulations on East African rainfall. Clim Dyn 56:2127-2147. https://doi.org/10.1007/s00382-020-05579-7

Tables

Type of simulation	Regional climate model	Lateral boundary conditions	Period of simulation
Evaluation simulation (EVAL)	KIT-CCLM5-0-15	ERA-Interim	19790102-20161231
	ICTP-RegCM4-7		19700101-20101130
	GERICS-REMO2015		19790102-20171231
Historical simulation (HIST)	KIT-CCLM5-0-15	MOHC-HadGEM2-ES	19500102-20051231
		MPI-M-MPI-ESM-LR	
		NCC-NorESM1-M	
	ICTP-RegCM4-7	MOHC-HadGEM2-ES	19700101-20051130
		MPI-M-MPI-ESM-MR	
		NCC-NorESM1-M	

	GERICS-REMO2015	MOHC-HadGEM2-ES	19700101-20051231
		MPI-M-MPI-ESM-LR	
		NCC-NorESM1-M	

Table 1 Overview of the simulations with the three different RCMs, driven by reanalysis and by the three different GCMs. In addition to the names of the models, identifiers for the modelling centres are given: the Karlsruhe Institute for Technology (KIT), Abdus Salam International Centre for Theoretical Physics (ICTP) and Climate Service Center Germany (GERICS) for the RCM simulations and the Met Office Hadley Centre for Climate Science and Services (MOHC), Max-Planck-Institute for Meteorology (MPI-M) and Norwegian Climate Centre (NCC) for the GCM simulations.

	Correlations								**Centred RMS deviations**							
RCM	**EVAL (1981-2009)**		**HIST (1981-2004)**						**EVAL (1981-2009)**		**HIST (1981-2004)**					
			HadGEM		**MPI-ESM**		**NorESM**				**HadGEM**		**MPI-ESM**		**NorESM**	
	1 rs	2rs	1 rs	2rs	1 rs	2 rs	1 rs	2 rs	1 rs	2 rs	1 rs	2 rs	1 rs	2 rs	1 rs	2 rs
CCLM	0.67	0.53	0.57	0.30	0.58	0.47	0.57	0.29	0.84	0.93	0.97	1.03	1.05	1.03	1.00	1.22
RegCM	0.80	0.68	0.71	0.20	0.72	0.56	0.72	0.28	0.73	0.82	0.90	1.36	0.88	0.92	0.86	1.40
REMO	0.69	0.46	0.58	0.15	0.64	0.38	0.59	0.20	0.75	0.96	0.87	1.27	0.79	1.04	0.85	1.26

Table 2 Medians of the correlations (left part) and the (normalized) centred root-mean-square deviations (right part) from the Taylor diagrams for the climatological annual cycle of daily precipitation for each grid point in the study region for the different RCM simulations with CHIRPS as reference data for 1981-2009 and 1981-2004, respectively, distinguishing between the grid points with one (1 rs) and two dominant rainy seasons (2 rs), respectively, dominate in CHIRPS. These are the evaluation simulations (EVAL) forced with ERA-Interim and the historical simulations (HIST) driven by the three different GCMs, i.e., HadGEM, MPI-ESM and NorESM, for the three different RCMs, i.e., CCLM, RegCM and REMO. For the corresponding histograms from the Taylor diagrams see Fig. 3 for the evaluation simulations and Figs. 5, S6 and S7 for the historical simulations, respectively.

Figures

The figures are provided in separate files.

Figure captions

Fig. 1 The study region, including 9 countries in East Africa: Eritrea (the border with Ethiopia is missing on the maps), Ethiopia, Djibouti, Somalia, Uganda, Kenya, Tanzania, Rwanda and Burundi, indicated by the topographic height. In-land water bodies in these countries are indicated in blue. Units are m; the contour interval is 100 m.

Fig. 2 The characteristics of the rainy seasons, i.e., the onset, cessation and length, from CHIRPS for 1981-2022, distinguishing between (a-c) one dominant rainy season, (d-f) the first and (g-i) the second of two dominant rainy seasons.

Grey in the study region indicates areas with neither one nor two dominant rainy seasons. Units are Julian day with a contour interval of 18 Julian days for the onset and cessation and day with a contour interval of 9 days for the length of the rainy seasons.

Fig. 3 Taylor diagrams (upper row) for the climatological annual cycle of daily precipitation for the RCM simulations forced with ERA-Interim (EVAL) for (a) CCLM, (b) RegCM and (c) REMO with CHIRPS as reference data for 1981-2009. All values, i.e., the centred root-mean-square deviation and the standard deviations of the data sets, are normalized by the standard deviation of CHIRPS. Also, histograms of the correlations (middle row) and centred root-means-square deviations (lower row) from the Taylor diagrams for (d, g) CCLM, (e, h) RegCM and (f, i) REMO, including the medians of the distributions (see Table 2). The red and blue colours indicate the grid points with one and two dominant rainy seasons, respectively, in CHIRPS. The values on the abscissa range between -0.2 and 1 standard units for the correlation and between 0.0 and 2.4 standard units for the (normalized) centred root-mean-square deviation. Units are %.

Fig. 4 Differences between the simulation with RegCM forced with ERA-Interim (EVAL) and CHIRPS in the characteristics of the rainy seasons, i.e., the onset, cessation and length, distinguishing between (a-c) one dominant rainy season, (d-f) the first and (g-i) the second of two dominant rainy seasons, for 1981-2009. Dark grey in the study region indicates areas with different dominant rainy seasons for the two datasets and light grey areas with neither one nor two dominant rainy seasons in one of the datasets. Units are day with a contour interval of 6 days.

Fig. 5 Taylor diagrams (upper row) for the climatological annual cycle of daily precipitation for the simulations with RegCM forced with (a) HadGEM, (b) MPI-ESM and (c) NorESM (HIST) with CHIRPS as reference data for 1981-2004. All values, i.e., the centred root-mean-square deviation and the standard deviations of the data sets, are normalized by the standard deviation of CHIRPS. Also, histograms of the correlations (middle row) and centred root-means-square deviations (lower row) from the Taylor diagrams for (d, g) HadGEM, (e, h) MPI-ESM and (f, i) NorESM, including the medians of the distributions (see Table 2). The red and blue colours indicate the grid points with one and two dominant rainy seasons, respectively, in CHIRPS, The values on the abscissa range between -0.2 and 1 standard units for the correlation and between 0.0 and 2.4 standard units for the (normalized) centred root-mean-square deviation. Units are %.

Fig. 6 Differences between the simulation with RegCM forced with HadGEM (HIST) and CHIRPS in the characteristics of the rainy seasons, i.e., the onset, cessation and length, distinguishing between (a-c) one dominant rainy season, (d-f) the first and (g-i) the second of two dominant rainy seasons, for 1981-2004. Dark grey in the study region indicates areas with different dominant rainy seasons for the two datasets and light grey areas with neither one nor two dominant rainy seasons in one of the datasets. Units are day with a contour interval of 6 days.

Fig. 7 As Fig. 6 but for the simulation forced with MPI-ESM.

Fig. 8 As Fig. 6 but for the simulation forced with NorESM.

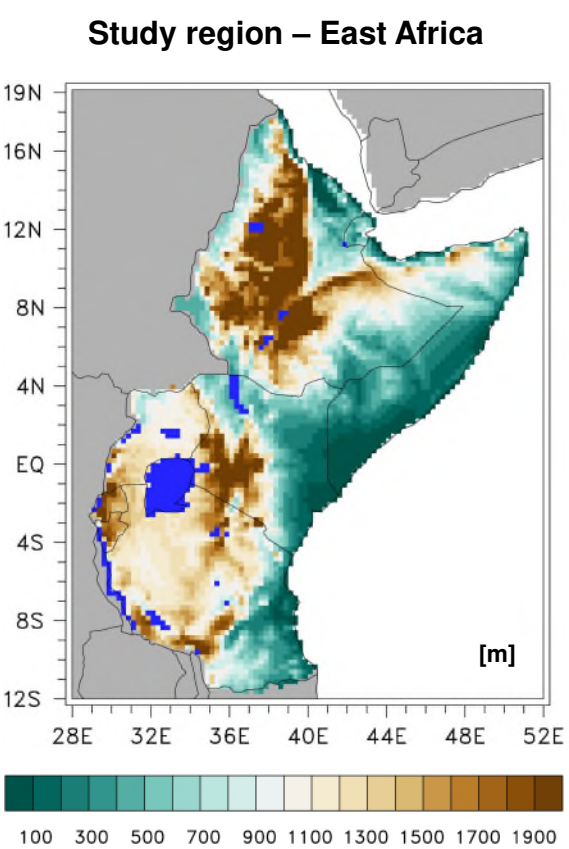


Fig. 1: The study region, including 9 countries in East Africa: Eritrea (the border with Ethiopia is missing on the maps), Ethiopia, Djibouti, Somalia, Uganda, Kenya, Tanzania, Rwanda and Burundi, indicated by the topographic height. In-land water bodies in these countries are indicated in blue. Units are m; the contour interval is 100 m.

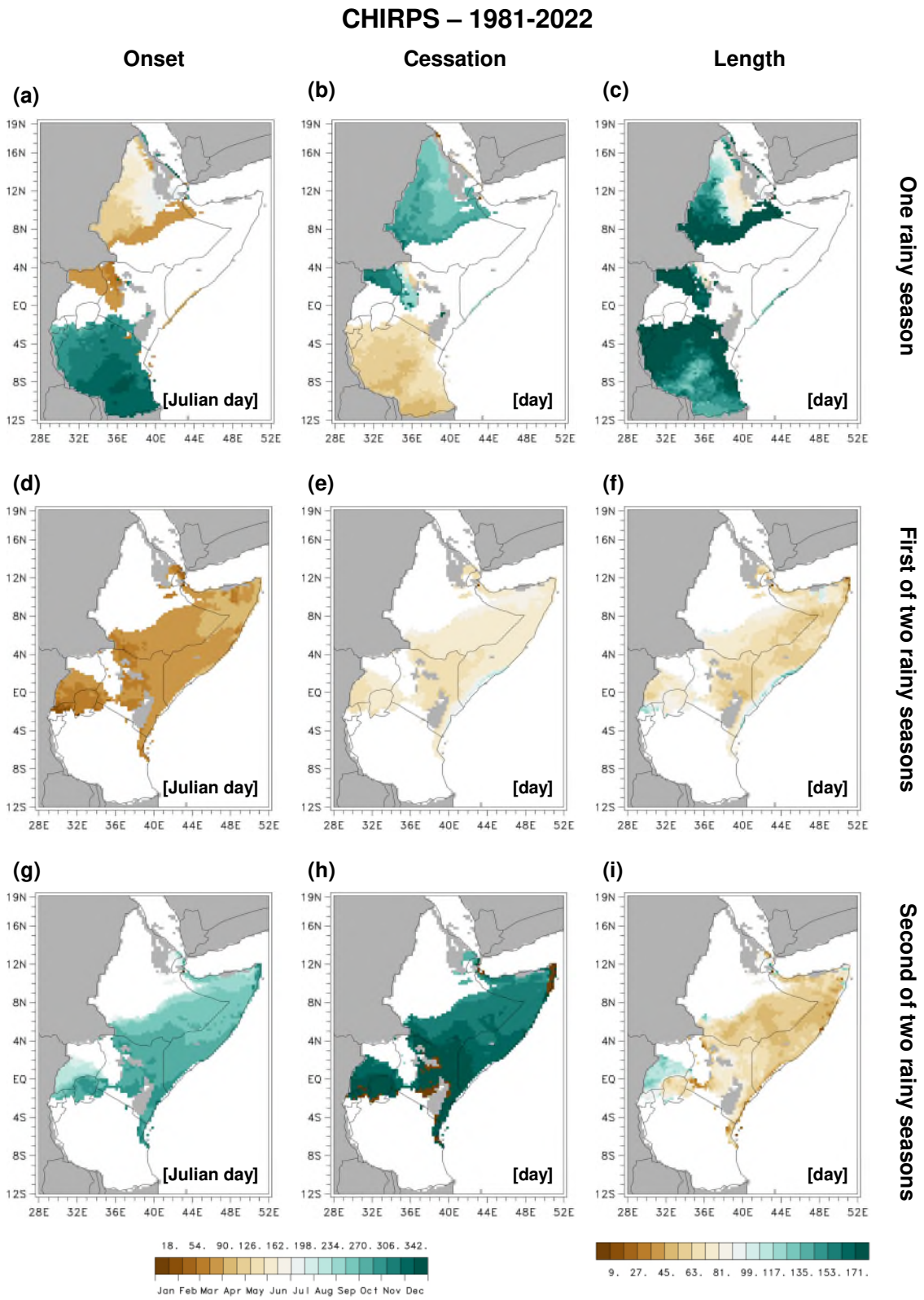


Fig. 2: The characteristics of the rainy seasons, i.e., the onset, cessation and length, from CHIRPS for 1981-2022, distinguishing between (a-c) one dominant rainy season, (d-f) the first and (g-i) the second of two dominant rainy seasons. Grey in the study region indicates areas with neither one nor two dominant rainy seasons. Units are Julian day with a contour interval of 18 Julian days for the onset and cessation and day with a contour interval of 9 days for the length of the rainy seasons.

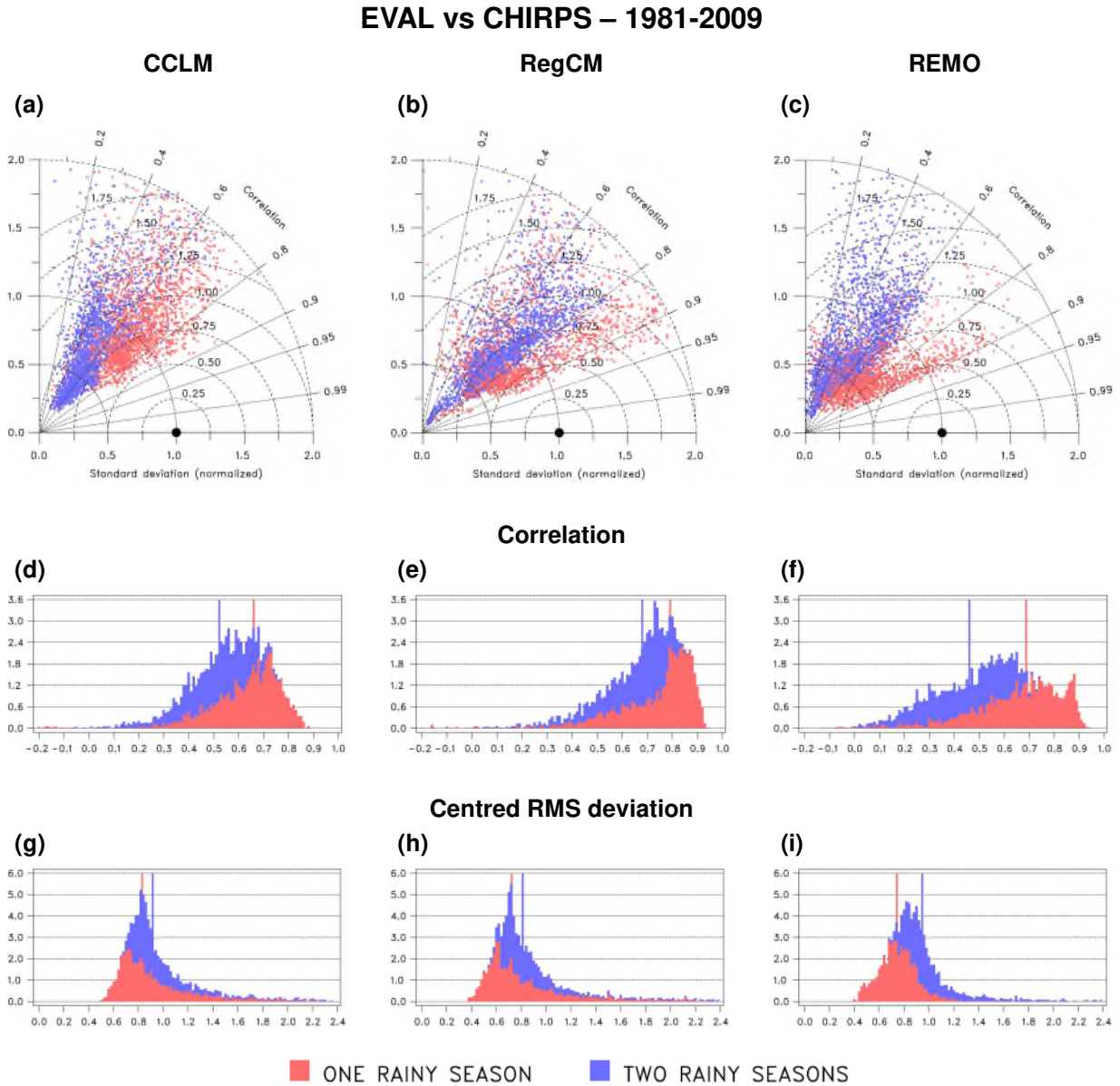


Fig. 3: Taylor diagrams (upper row) for the climatological annual cycle of daily precipitation for the RCM simulations forced with ERA-Interim (EVAL) for (a) CCLM, (b) RegCM and (c) REMO with CHIRPS as reference data for 1981-2009. All values, i.e., the centred root-mean-square deviation and the standard deviations of the data sets, are normalized by the standard deviation of CHIRPS. Also, histograms of the correlations (middle row) and centred root-means-square deviations (lower row) from the Taylor diagrams for (d, g) CCLM, (e, h) RegCM and (f, i) REMO, including the medians of the distributions (see Table 2). The red and blue colours indicate the grid points with one and two dominant rainy seasons, respectively, in CHIRPS. The values on the abscissa range between -0.2 and 1 standard units for the correlation and between 0.0 and 2.4 standard units for the (normalized) centred root-mean-square deviation. Units are %.

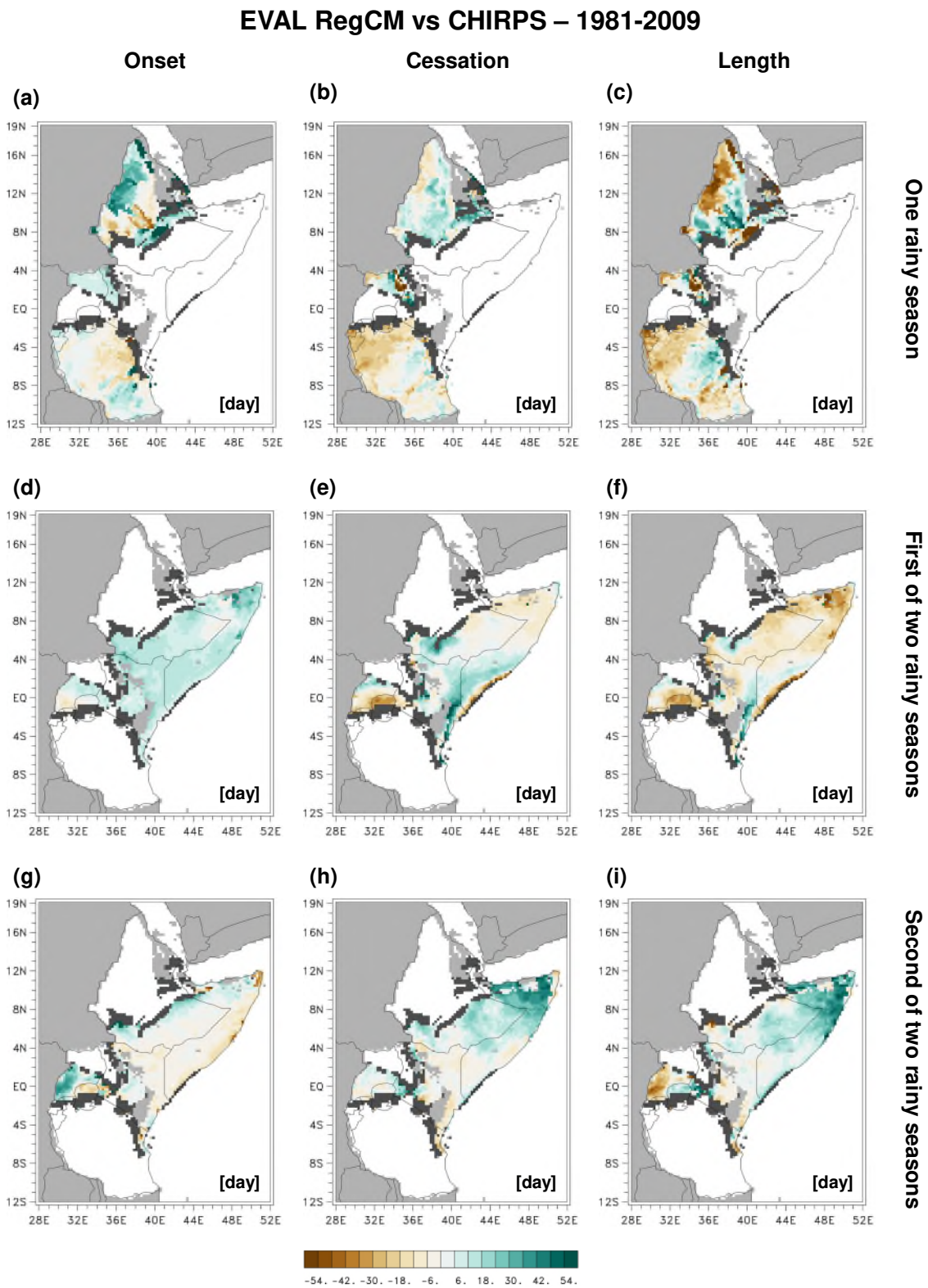


Fig. 4: Differences between the simulation with RegCM forced with ERA-Interim (EVAL) and CHIRPS in the characteristics of the rainy seasons, i.e., the onset, cessation and length, distinguishing between (a-c) one dominant rainy season, (d-f) the first and (g-i) the second of two dominant rainy seasons, for 1981-2009. Dark grey in the study region indicates areas with different dominant rainy seasons for the two datasets and light grey areas with neither one nor two dominant rainy seasons in one of the datasets. Units are day with a contour interval of 6 days.

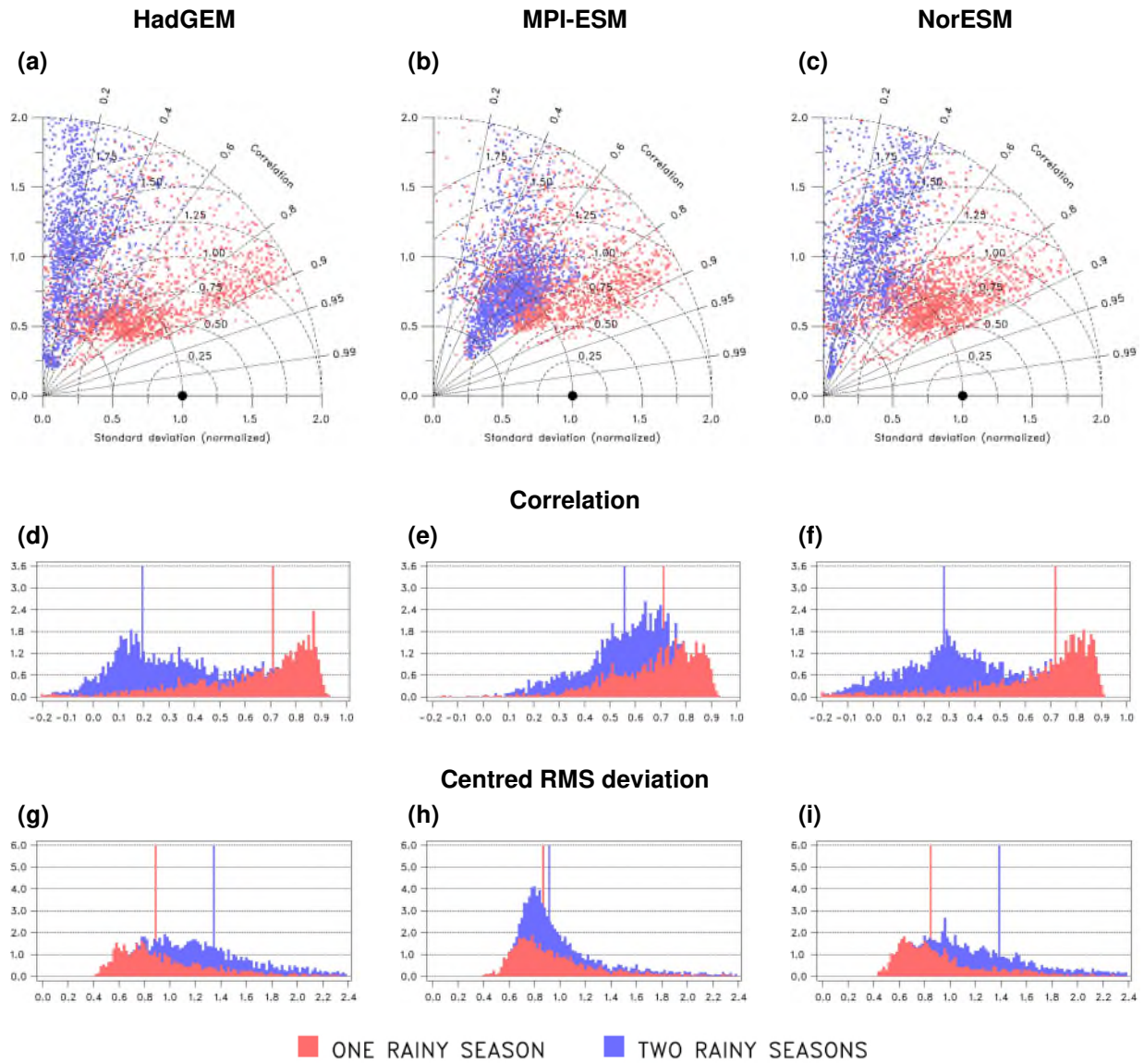


Fig. 5: Taylor diagrams (upper row) for the climatological annual cycle of daily precipitation for the simulations with RegCM forced with (a) HadGEM, (b) MPI-ESM and (c) NorESM (HIST) with CHIRPS as reference data for 1981-2004. All values, i.e., the centred root-mean-square deviation and the standard deviations of the data sets, are normalized by the standard deviation of CHIRPS. Also, histograms of the correlations (middle row) and centred root-means-square deviations (lower row) from the Taylor diagrams for (d, g) HadGEM, (e, h) MPI-ESM and (f, i) NorESM, including the medians of the distributions (see Table 2). The red and blue colours indicate the grid points with one and two dominant rainy seasons, respectively, in CHIRPS. The values on the abscissa range between -0.2 and 1 standard units for the correlation and between 0.0 and 2.4 standard units for the (normalized) centred root-mean-square deviation. Units are %.

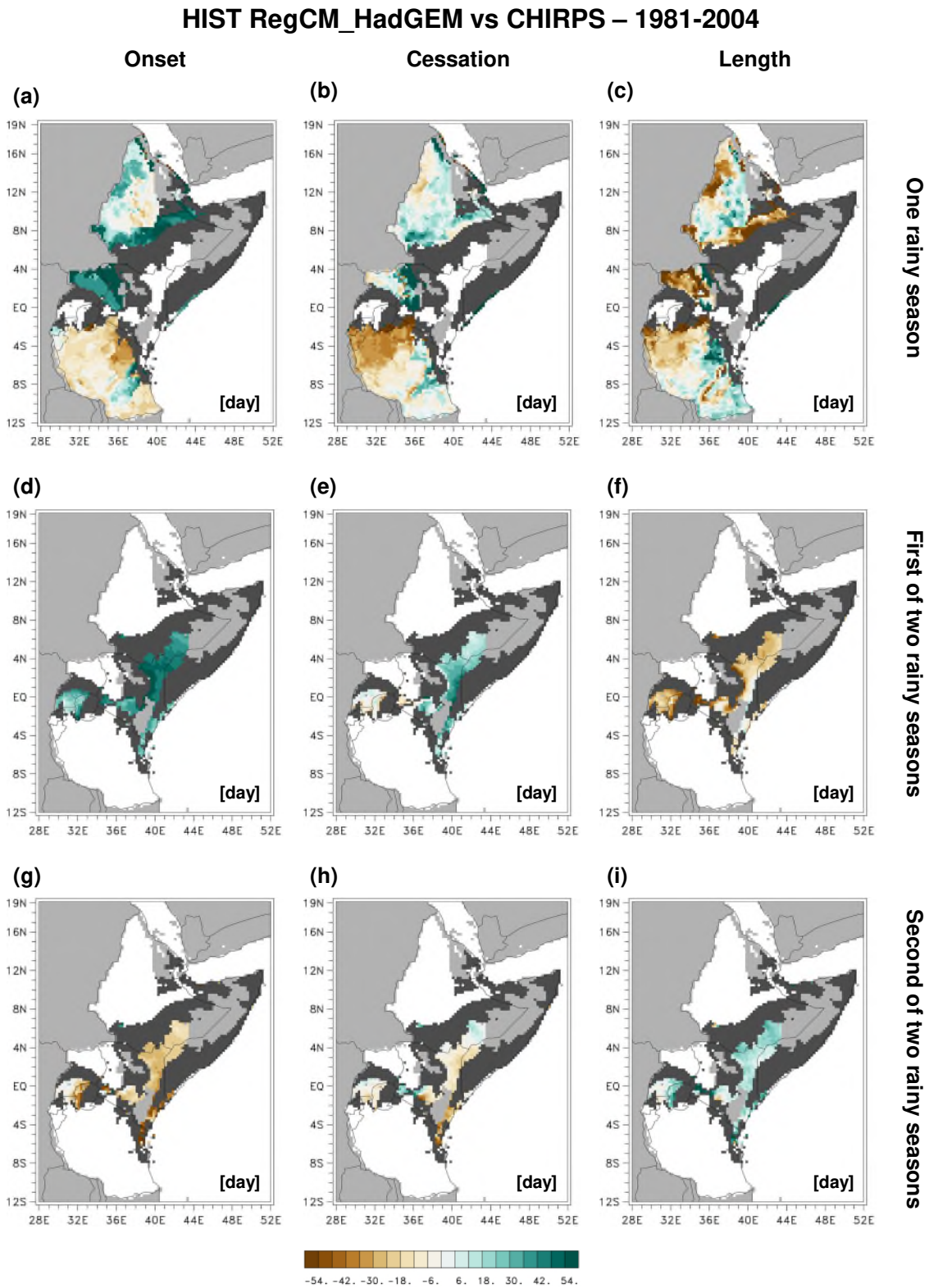


Fig. 6: Differences between the simulation with RegCM forced with HadGEM (HIST) and CHIRPS in the characteristics of the rainy seasons, i.e., the onset, cessation and length, distinguishing between (a-c) one dominant rainy season, (d-f) the first and (g-i) the second of two dominant rainy seasons, for 1981-2004. Dark grey in the study region indicates areas with different dominant rainy seasons for the two datasets and light grey areas with neither one nor two dominant rainy seasons in one of the datasets. Units are day with a contour interval of 6 days.

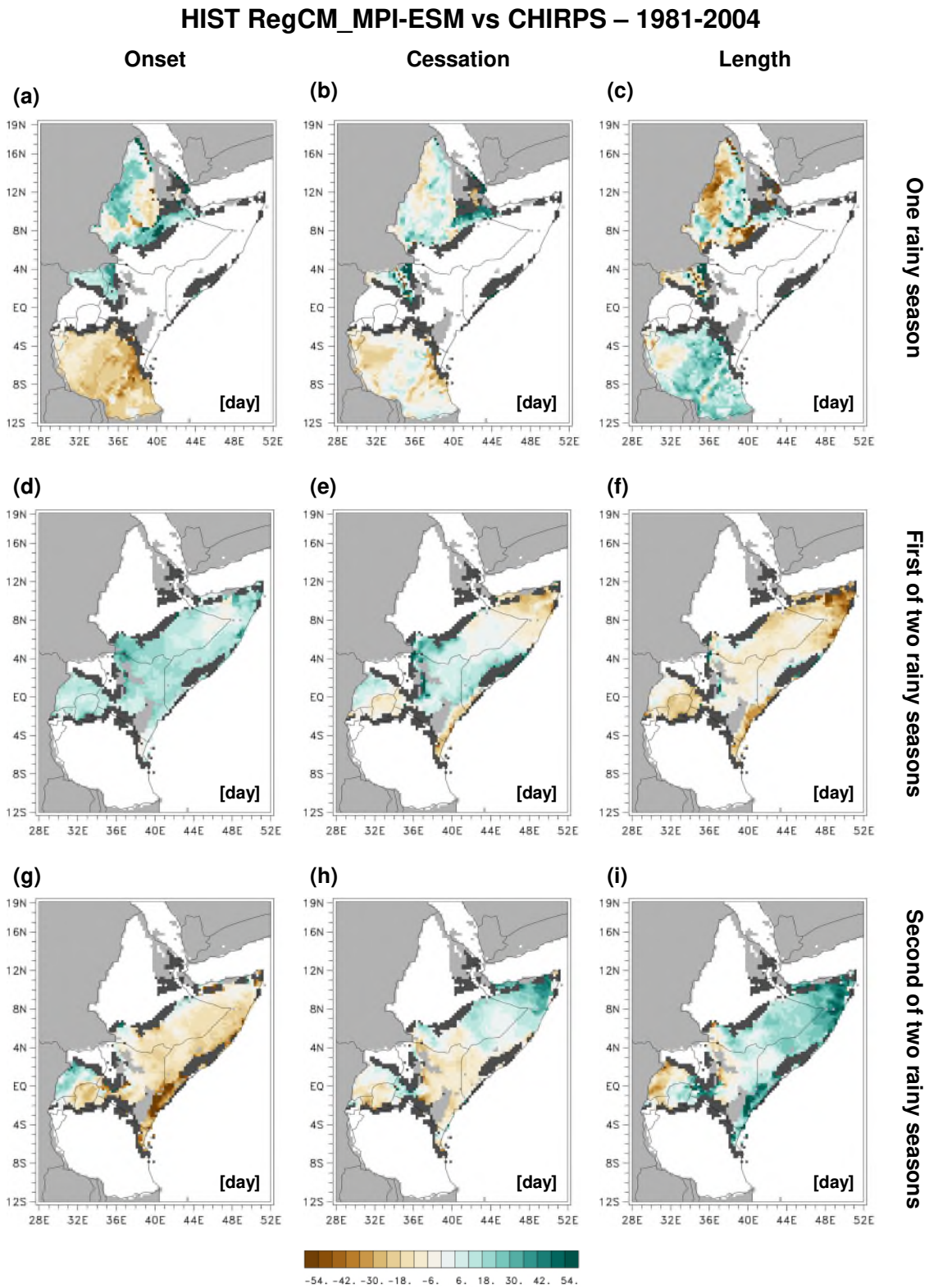


Fig. 7: As Fig. 6 but for the simulation forced with MPI-ESM.

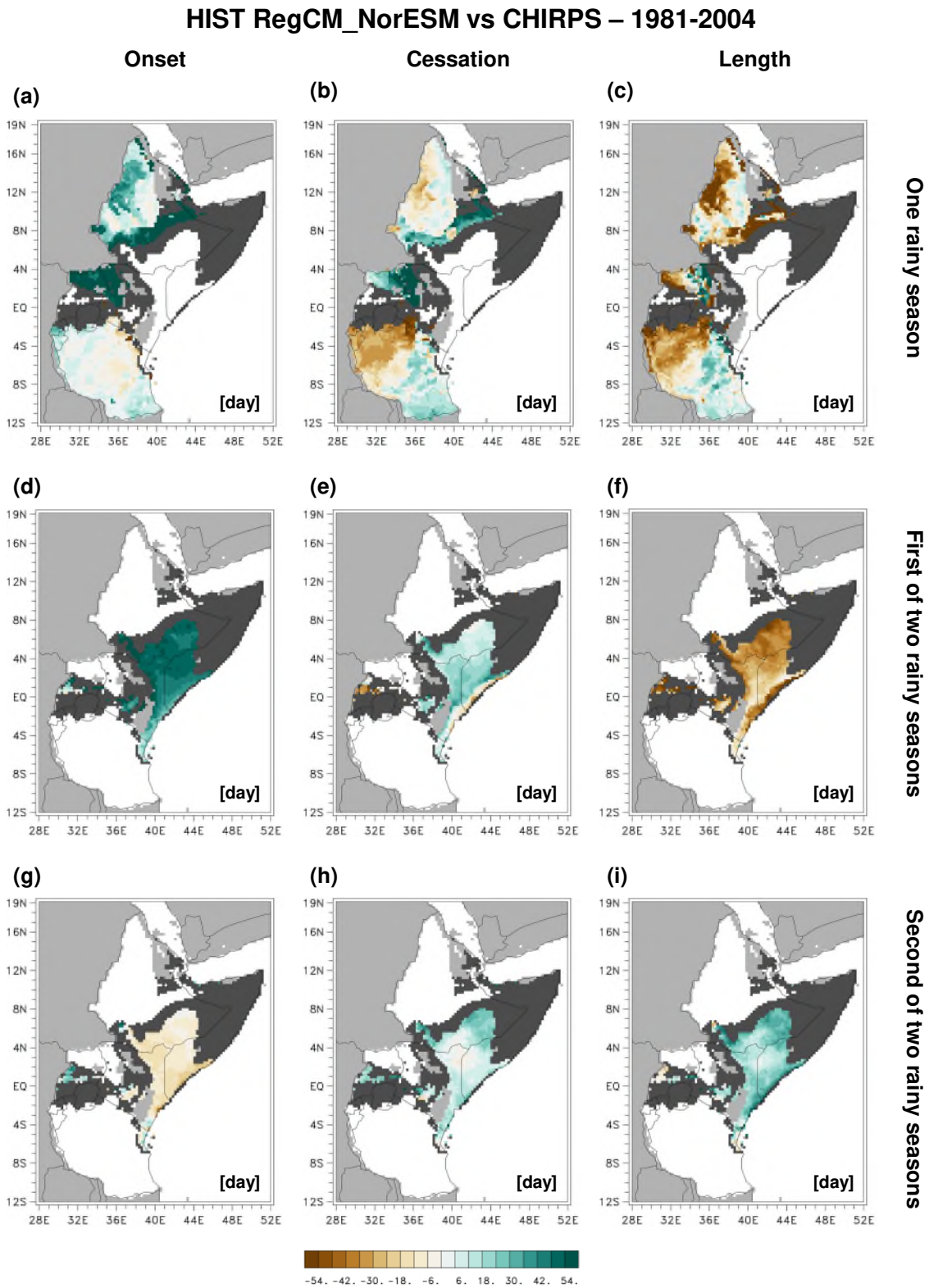


Fig. 8: As Fig. 6 but for the simulation forced with NorESM.

Supplementary Files

This is a list of supplementary files associated with this preprint. Click to download.

- May2026suppl20261028.docx